# Inhibition of Histamine H3 receptor Attenuates Neuroinflammation and Cognitive Impairments in Alzheimer's Disease via activating CREB Pathway

**Jiangong Wang**
Binzhou Medical University
**Bin Liu**
Binzhou Medical University
**Yong Xu**
Binzhou Medical University
**Chaoyun Wang**
Binzhou Medical University
**Meizi Yang**
Binzhou Medical University
**Mengmeng Song**
Dongying People's Hospital
**Jing Liu**
Binzhou Medical University
**Jingjing You**
Binzhou Medical University
**Fengjiao Sun**
Binzhou Medical University
**Wentao Wang**
Binzhou Medical University
**Haijing Yan** ( hjyan211@163.com )
Binzhou Medical University https://orcid.org/0000-0002-0997-5299

**Research**

**Keywords:** Histamine, Histamine H3 receptor, Thioperamide, Alzheimer's disease, Cognitive impairment, β-amyloid, Microglia, Astrocyte, Gliosis, Cyclic AMP response element-binding protein, Nuclear factor kappa-B, Interleukin-1β, Tumor necrosis factor α, Interleukin-4

**Posted Date:** December 16th, 2020

**DOI:** https://doi.org/10.21203/rs.3.rs-126764/v1

# Abstract

Background

Alzheimer's disease (AD) is an age-related neurodegenerative disease, which characterized by deposition of amyloid-β (Aβ) plaques, neurofibrillary tangles, neuronal loss, and accompanied by neuroinflammation. Neuroinflammatory processes are well acknowledged to contribute to the progression of AD pathology. Histamine H3 receptor (H3R) is a presynaptic autoreceptor regulating histamine release via negative feedback way. H3R antagonist has been reported to have anti-inflammatory efficacy. However, whether inhibition of H3R is responsible for the anti-neuroinflammation and neuroprotection on APP/PS1 Tg mice remains unclear.

Methods

In this study, microgliosis, astrogliosis, A1 type astrocytes and A2 type astrocytes in APP/PS1 Tg mice were measured by immunostaining by Iba1, GFAP, C3 and S100A10 with and without treatment of thioperamide, an H3R antagonist. Inflammatory response of APP/PS1 Tg mice and effects of thioperamide were studied by measuring levels of pro-inflammatory cytokines (tumor necrosis factor α [TNFα] and interleukin-1β [IL-1β]) and anti-inflammatory cytokines (interleukin-4 [IL-4]). Protein levels of p-CREB and p-P65 NF-kB was tested by western blot to study the mechanism of thioperamide on AD. H89 was applied to study whether the mechanism offered by thioperamide was dependent on CREB activating. The effect of thioperamide and H89 on Aβ deposition was measured by immunostaining and ELISA. The cognitive function was tested by novel object recognition, Y maze and morris water maze.

Results

Inhibition of H3R by thioperamide reduced the gliosis and induced a phenotypical switch from A1 to A2 in astrocytes, and ultimately attenuated neuroinflammation in APP/PS1 Tg mice. Additionally, thioperamide rescued the decrease of cyclic AMP response element-binding protein (CREB) phosphorylation and suppressed the phosphorylated nuclear factor kappa B (NF-κB) in APP/PS1 Tg mice. H89, an inhibitor of CREB signaling, abolished these effects of thioperamide to suppress gliosis and proinflammatory cytokine release. Lastly, thioperamide alleviated the deposition of Aβ and cognitive dysfunction in APP/PS1 mice, which were both reversed by administration of H89.

Conclusions

Taken together, these results suggested the H3R antagonist thioperamide improved cognitive impairment in APP/PS1 Tg mice via modulation of the CREB-mediated gliosis and inflammation inhibiting, which contributed to Aβ clearance. This study uncovered a novel mechanism involving inflammatory regulating behind the therapeutic effect of thioperamide in AD.

# Background

Alzheimer's disease (AD) is an age-related, progressive neurodegenerative disease which pathologically characterized by the presence of extracellular amyloid-β (Aβ)-containing senile plaques and intracellular hyperphosphorylated tau-containing neurofibrillary tangles, neuroinflammation, synaptic loss and neuronal death, neocortical atrophy and the progressive deterioration of cognitive function[1-4]. The deposition of extracellular Aβ is the primary influence driving AD pathogenesis [5]. Microglia and astrocytes play a major role in regulating neuroinflammation and the deposition of Aβ [6]. Overactivation of glial cells leads to excessive release of proinflammatory factors such as IL-1β and TNF-α, which also contributes to the deposition of Aβ and the progression of AD [7-9]. However, moderate activation of glial cells plays an important role in the clearance of Aβ via induction of phagocytosis and autophagy [10, 11], suggesting a dual role for neuroinflammation on Aβ pathology in AD. Emerging studies have demonstrated that controlling microglial and astrocyte activation-mediated neuroinflammation is an important therapeutic strategy for AD treatment [12, 13]. In fact, the anti-inflammatory agents should be beneficial in delaying the onset or slowing the progression of AD. However, it is still far from conclusive results for a majority of mixed and contradictory results [14, 15]. Therefore, it is of great importance to develop some new and more specific anti-inflammatory agents.

Histamine is an endogenous neurotransmitter in the brain [16] . Up to now, there are four subtypes of receptors have been identified: H1R, H2R, H3R and H4R, of which H1R–H3R are found in brain [17-19]. Histamine H3 receptor (H3R) is a presynaptic autoreceptor that regulates histamine release from histaminergic neurons via negative feedback way [20, 21], as well as a heteroreceptor that regulates the release of other neurotransmitters [22-27]. H3R is a G-protein-coupled receptor (GRCR) that activates Gi/o proteins to inhibit adenylyl cyclase (AC) and cAMP-response element binding protein (CREB) activity [28]. A number of experiments have provided evidences that inhibition of H3R could alleviate cognitive deficit in AD [29-32]. Therefore, it raises the possibility of H3R antagonist for AD treatment. However, the potential mechanisms remain to be clarified. Previous studies have shown that H3R antagonist rescues autistic spectrum disorder-like behaviors through attenuating the proinflammatory cytokines [33]. Thioperamide, a histamine H3R antagonist, also suppresses inflammatory cell recruitment after ischemic events through histamine dependent mechanism [34]. In addition, activation of H3R downstream signaling CREB, which is involved in improving cognitive dysfunction and Aβ pathology in AD [35, 36], could also suppresses inflammatory response [37-39] through inhibiting the activation of glial cells [40-42]. Nevertheless, whether CREB-mediated anti-inflammation and inactivation of glial cells are involved in the alleviated cognitive deficit and Aβ pathology by H3R antagonist in AD remains undetermined.

In this study, we hypothesize that inhibition of H3R may reduce the AD-related Aβ pathology and improve cognitive dysfunction through suppressing overactivation of glial cells-induced inflammatory response via CREB/NF-κB pathway. We would show the beneficial effect of H3R antagonist and explain a novel mechanism that H3R antagonist-mediated effect of anti-inflammation in AD.

# Methods

### Ethical statement

All animal studies were carried out according to protocols approved by the Institutional Animal Care and Use Committee of Binzhou Medical University, and conducted in compliance with the National Institutes of Health Guide for the Care and Use of Laboratory Animals. Efforts were made to minimize any pain or discomfort, and the minimum number of animals was used.

### Animals

Adult male wild type (WT) and BL/6-Tg (APPswe, PSEN1dE9) (APP/PS1) mice of 9 months (from Jackson Lab, Stock Number: 004462) were used in this study. The mice were housed in a temperature- and humidity-controlled animal facility, which was maintained on a 12 h light/dark cycle, food and water were given *ad libitum*.

### Stereotaxic surgery

Stereotaxic surgery was performed as previously described [43]. Mice were anesthetized with the intraperitoneal injection of 1% chloral hydrate and then immobilized on a stereotactic frame. The gauge guide cannula was implanted into the lateral ventricle (0.2 mm posterior, 1.1 mm lateral and 2.7 mm ventral to the bregma). After surgery, mice were housed individually and allowed to recover for 7 d.

### Drug treatments

For *in vivo* study, a stainless-steel injector connected to a 5-μl syringe was inserted into the guide cannula and extended 1 mm beyond the tip. The administration of the chemicals was administrated on the basis of previous studies [44]. Thioperamide (i.p., 5 mg/kg) or vehicle was administrated daily at 7 days after stereotaxic surgery until the beginning of the behavior tests on day 14. H89 or vehicle (*i.c.v.*, 5 μM of 2 μl) was administrated 0.5 h before thioperamide injection. Thioperamide and H89 were dissolved in saline. At 14 days after stereotaxic surgery, the novel object recognition (NOR) test was carried on for 4 days. At 18 days after stereotaxic surgery, Y maze (YM) test was carried on for 1 day. At 19 days after stereotaxic surgery, morris water maze (MWM) test was carried on for 6 days. During the period of behavior test, thioperamide or vehicle was administrated 0.5 h, whereas H89 or vehicle was administrated 1 h before the test at day 14, day 18 and day 19.

### Immunohistochemistry

Immunostaining was performed in frozen brain sections. Frozen brain sections were fixed in 4% paraformaldehyde for 2 h, and then incubated in 5% bovine serum albumin (BSA, Solarbio) for 2 h to block nonspecific binding of IgG. Then the cells were reacted with mouse antibody against GFAP (1:400; 3670, Cell signaling technology), goat antibody against Iba1 (1:300; ab5076, Abcam), rabbit antibody against GFAP (1:200; bm4287, Boster), C3 (1:100; ab200999, abcam), S100A10 (1:200; ab76472, Abcam), phospho-CREB (9198, Cell Signaling Technology, 1:1,000), CREB (9197, Cell signaling technology, 1:1,000), Aβ (ab201060, 1:100, Abcam). After repeated washes in PBS buffer, cells were incubated with secondary antibody in 3% BSA for 2 h at 25°C. The secondary antibodies used in this experiment were donkey anti-mouse IgG-AlexaFluo 488 (1:300, 21202, Invitrogen), goat anti-rabbit IgG-AlexaFluo 546

(1:300, A11035, Invitrogen), goat anti-rabbit IgG-AlexaFluo 647 (1:300, A21245, Invitrogen), goat anti-mouse IgG-AlexaFluo 647 (1:300, A21236, Invitrogen), donkey anti-rabbit IgG-AlexaFluo 488 (1:300, A21206, Invitrogen), goat anti-mouse IgG-AlexaFluo 546 (1:300, A11030, Invitrogen), and donkey anti-goat IgG-AlexaFluo 546 (1:300, A11056, Invitrogen). After further washing in PBS, cultures were dried, cover slipped and mounted on glass slides. For thioflavin S staining, sections were incubated with 70 and 80% ethanol and stained with 1% thioflavin S (Sigma) in 80% ethanol for 15 min. Afterward, sections were rinsed in 80% and 70% ethanol and distilled water. The stained cells were observed under a laser scanning confocal microscope (Leica TCS SPE, Germany). All the immunohistochemical data represent mean values of 5 brain sections per mouse. The plaque and Aβ area coverage as well as the number of Iba1-positive, GFAP-positive cells were quantified using ImageJ. The numbers of near-plaque Iba1- and GFAP-positive cells were defined as near-plaque when they were located ≤ 50 μm around plaques.

### ELISA

Mice were anaesthetized by i.p. injection of chloral hydrate (400 mg/kg), sacrificed and the brain was quickly removed. The separated tissues were lysed in ice-cold RIPA lysis buffer (R0020, Solarbio), then centrifuged at 14,000×g at 4°C for 20 min, and the supernatants were measured for soluble Aβ40, Aβ42, IL-1β, TNF-α and IL-4 ELISAs (R&D) according to the manufacturer's instructions. The values were expressed as amount per total protein.

### Western blot

Western blot was performed as previously described [45]. Briefly, mice were anaesthetized by i.p. injection of chloral hydrate (400 mg/kg), sacrificed and the brain was quickly removed. The separated tissues were lysed in ice-cold RIPA lysis buffer (R0020, Solarbio), then centrifuged at 14,000×g at 4°C for 20 min, and the protein concentration in the extracts was determined by the Bradford assay (Thermo, Hercules, CA). The precipitates were denatured with SDS sample loading buffer and separated on 10% SDS-PAGE. Proteins were transferred onto nitrocellulose membranes using a Bio-Rad mini-protein-III wet transfer unit overnight at 4°C. Transfer membranes were then incubated with blocking solution (5% nonfat dried milk dissolved in tris buffered saline tween (TBST) buffer (in mM): 10 Tris-HCl, 150 NaCl, and 0.1% Tween-20) for 2 h at room temperature, and incubated with primary antibody overnight at 4°C. The primary antibodies used in this experiment were phospho-CREB (Cell Signaling Technology, 1:1,000), CREB (Cell Signaling Technology, 1:1,000), p-P65 NF-kB (abcam, 1:1000), P65 NF-kB (abcam, 1:1000) and GAPDH (Kangchen Biotech, 1:3,000). Membranes were washed three times in TBST buffer and incubated with the appropriate secondary antibodies (LI-COR, Odyssey, 1:5,000) for 2 h. Images were acquired with the Odyssey infrared imaging system and analyzed as specified in the Odyssey software manual. The results were expressed as the target protein/GAPDH ratio and then normalized to the values measured in the control groups (presented as 100%).

### Novel object recognition (NOR)

The NOR test was performed 14 days after stereotaxic surgery as previously described [43, 46]. Briefly, mice received 2 d of habituation in a 45 × 45 cm square arena, and on the third day, they were allowed to explore two identical objects made from large Lego bricks for 10 min (training trial). They were returned to their home cage, and 24 h later, a different shape and color object replaced one of the objects and the mice were returned to the arena for 10 min (testing trial). The time spent on each object was then calculated as a percentage of total object exploration.

### Y maze (YM)

The Y maze test was performed 18 days after stereotaxic surgery as previously described [43, 46]. Briefly, the apparatus for YM was made of gray plastic, with each arm 40 cm long, 12 cm high, 3 cm wide at the bottom and 10 cm wide at the top. The three arms were connected at an angle of 120°. Mice were individually placed at the end of an arm and allowed to explore the maze freely for 8 min. The total arm entries and spontaneous alternation percentage (SA%) were measured. SA% was defined as a ratio of the arm choices that differed from the previous two choices ('successful choices') to total choices during the run ('total entry minus two' because the first two entries could not be evaluated). For example, if a mouse made 10 entries, such as 1-2-3-2-3-1-2-3-2-1, there are 5 successful choices in 8 total choices (10 entries minus 2). Therefore, SA% in this case is 62.5%.

### Morris water maze (MWM)

The MWM maze test was performed 19 days after stereotaxic surgery as previously described [43, 47]. Briefly, the water maze of 1.50 m in diameter and 0.50 m in height was filled with water (20 ± 1°C) to maintain the water surface 1.50 cm higher than the platform (10 cm in diameter). Water was dyed white and the tank was divided into four quadrants by four points: North (N), South (S), East (E), and West (W). The platform was placed at the center of either quadrant and video tracking software was used to automatically track the animals. Learning and memory acquisition lasts for five days. Animals were put into the water from four points in random order every day until they found the platform and stayed for 10 s within 1 min. If the mice cannot find the platform within 1 min, they were guided to the platform. Following acquisition test, on the sixth day, learning and memory maintenance test was carried on. The platform was removed, and the mice were placed in water from the opposite quadrant of the platform, and then the times crossing the platform was recorded within 1 min.

### Statistical analysis

Results are expressed as mean ± SEM. Statistical analysis was performed by one-way ANOVAs followed by Tukey's *post hoc* comparisons or two-way ANOVAs followed by Bonferroni *post hoc* comparisons, using prism software. *P* value <0.05 was considered statistically significant.

## Results

### Thioperamide decreases the microglial reactivity in APP/PS1 Tg mice

We used 8-month-old APP/PS1 Tg mice which have the mutated human APPswe and PSEN1ΔE9, to examine the therapeutic efficacy of thioperamide, a H3R antagonist in AD. Activated microglia may play an important role in the pathogenesis of AD as they cluster around Aβ plaques [48]. Therefore, we examined the activated microglia in the hippocampus and cortex by Iba1 immunostaining. Results showed that the area of $Iba1^+$-cells in the whole hippocampus, hippocampal CA1, CA3 and DG of APP/PS1 Tg mice increased dramatically compared with the WT mice (from 0.8422 ± 0.1892 to 5.012 ± 0.8202, $P$ <0.001; from 0.9386 ± 0.1078 to 4.403 ± 0.6446, $P$ <0.001; from 0.8750 ± 0.03305 to 6.096 ± 0.4614, $P$ <0.001; from 1.119 ± 0.1738 to 4.730 ± 0.3491, $P$ <0.001, respectively, Fig. 1A-E), which was reversed by administration of thioperamide (to 2.280 ± 0.4046, $P$ <0.01; to 1.987 ± 0.4507, $P$ <0.01; to 1.821 ± 0.2154, $P$ <0.001; to 1.834 ± 0.3491, $P$ <0.001, respectively, Fig. 1A-E). Similarly, we also observed a decrease of $Iba1^+$-cells in the cortex with administration of thioperamide compared with the vehicle-treated APP/PS1 mice (from 3.262 ± 0.6586 to 1.596 ± 0.1891, $P$ <0.01, Fig. 1A, F). Moreover, we examined the number of $Iba1^+$-cells around the plaques in the hippocampus and cortex. Results showed that thioperamide treatment significantly inhibited the clustering microglia around the plaques staining with Thioflavin S (from 7.000 ± 0.9487 to 3.400 ± 0.5099 in hippocampus, $P$ <0.05; from 6.400 ± 0.8124 to 2.600 ± 0.4000 in cortex, $P$ <0.01, Fig. 1A, G, H). These data suggested that APP/PS1 Tg mice induced an increased activation of microglia in the hippocampus and cortex. Thioperamide treatment resulted in suppressed activation and decreased clustering microglia around plaques in APP/PS1 Tg mice.

### Thioperamide decreases the astrocytic reactivity in APP/PS1 Tg mice

In AD, microglia produces an array of pro-inflammatory cytokines and mediators in response to Aβ. This in turn activates astrocytes. Activated astrocytes in AD become a part of the inflammatory process when, in addition to microglia [49]. Therefore, we also evaluated astrogliosis, another pathological hallmark of AD. We found that APP/PS1 Tg mice showed stronger GFAP immunoreactivities in the whole hippocampus, hippocampal CA1, CA3, DG and cortex (from 0.6240 ± 0.0598 to 2839 ± 0.2192, $P$ <0.001; from 0.6180 ± 0.09044 to 3.797 ± 0.6703, $P$ <0.001; from 0.5913 ± 0.039059 to 3.917 ± 0.4596, $P$ <0.001; from 0.6945 ± 0.07266 to 3.297 ± 0.7220, $P$ <0.05; from 0.2613 ± 0.06796 to 1.979 ± 0.1788, $P$ <0.001, respectively, Fig. 2A-F), suggestive of increased astrogliosis. As expect, thioperamide treatment inhibited the astrogliosis in either hippocampus (to 1.333 ± 0.1862 in whole hippocampus, $P$ <0.001; to 1.397 ± 0.1554 in hippocampal CA1, $P$ <0.01; to 1.264 ± 0.2338 in hippocampal CA3, $P$ <0.001; to 1.051 ± 0.3235 in hippocampal DG, $P$ <0.05, Fig. 2A-E) or cortex (to 0.8285 ± 0.1243, $P$ <0.001, Fig. 2F). In addition, the number of activated astrocytes around the plaques in the hippocampus was also assessed. Results showed that thioperamide treatment significantly inhibited the clustering astrocytes around the plaques (from 9.200 ± 0.4899 to 5.600 ± 0.6782, $P$ <0.01, Fig. 3A, B). Above all, these results suggested that thioperamide inhibited the astrogliosis and astrocytes clustering around the plaques in APP/PS1 Tg mice.

### Thioperamide induces a phenotypical switch in astrocytes in APP/PS1 Tg mice

There is an A1/A2 nomenclature for astrocytes to characterize pro-inflammatory and anti-inflammatory effects respectively. Accordingly, toxic reactive astrocytes would be termed as “A1 astrocytes” and

protective reactive astrocytes as “A2 astrocytes” [50]. Activated microglia secrets pro-inflammatory cytokines to induce A1 astrocytes, which lose most normal astrocytic functions but gain a new neurotoxic function [51]. In order to investigate the effect of thioperamide on the neurotoxic A1 astrocytes in AD, complement 3 (C3), a protein marker of A1 astrocytes was co-stained with GFAP. The results indicated that thioperamide significantly decreased the number of neurotoxic $C3^+/GFAP^+$ astrocytes in hippocampus (decreased to 51.95 ± 10.27% of vehicle group, $P$ <0.05, Fig. 3C, D). In order to investigate the effect of thioperamide on protective A2 astrocytes, S100A10, a protein marker of A2 astrocytes was co-immunostained with GFAP. Interestingly, the number of A2 type protective astrocytes increased markedly in the thioperamide treated group compared with the vehicle group (increased to 211.1 ± 25.76% of vehicle group, $P$ <0.01, Fig. 3E, F). Taken together, these results indicated that thioperamide induced an A1-to-A2 switch in astrocytes.

### Thioperamide decreases pro-inflammatory cytokines production in APP/PS1 Tg mice

The activation of microglia and A1 type astrocytes may promote the pathological process through releasing of pro-inflammatory cytokines [51, 52], which could lead to neuronal damage and cognitive impairments. Moreover, the inflammatory cytokines in AD lesions are thought to lead to an increased accumulation of Aβ production [12]. Therefore, we investigated expression of pro-inflammatory factors associated with Aβ accumulation, including IL-1β, TNF-α and IL-4 in APP/PS1 Tg mice and WT mice. Our results showed that the levels of IL-1β and TNF-α increased markedly (from 380.1 ± 33.44 to 550.9 ± 26.67 in hippocampus of IL-1β, $P$ <0.01, Fig. 4A; from 399.3 ± 29.80 to 582.2 ± 34.54 in cortex of IL-1β, $P$ <0.01, Fig. 4B; from 708.8 ± 39.15 to 921.2 ± 17.23 in hippocampus of TNFα, $P$ <0.01, Fig. 4C; from 713.8 ± 40.14 to 927.5 ± 40.25 in cortex of TNFα, $P$ <0.05, Fig. 4D), whereas IL-4 remained unchanged in either hippocampus or cortex in APP/PS1 Tg mice compared with the WT mice (from 310.1 ± 38.33 to 336.2 ± 18.95 in hippocampus, $P$ >0.05, Fig. 4E; from 315.6 ± 28.88 to 337.62 ± 26.00 in cortex, $P$ >0.05, Fig. 4F). Interestingly, the levels of inflammatory cytokines IL-1β and TNF-α were dramatically decreased in both hippocampus and cortex in thioperamide-treated APP/PS1 Tg mice (decreased to 390.9 ± 27.33 in hippocampus of IL-1β, $P$ <0.01, Fig. 4A; decreased to 408.9 ± 29.31 in cortex IL-1β, $P$ <0.01, Fig. 4B; decreased to 722.5 ± 54.57 in hippocampus of TNF-α, $P$ <0.05, Fig. 4C; decreased to 727.5 ± 48.21 in cortex of TNF-α, $P$ <0.05, Fig. 4D). Moreover, the anti-inflammatory mediator IL-4 increased significantly in both the hippocampus and cortex of thioperamide-treated APP/PS1 mice compared with the APP/PS1 Tg controls (increased to 485.1 ± 44.52 in hippocampus, $P$ <0.05, Fig. 4E; decreased to 490.5 ± 32.10 in cortex, $P$ <0.01, Fig. 4F). All these results suggested that thioperamide could effectively suppress the secretion of inflammatory cytokines in APP/PS1 Tg mice.

### Thioperamide up-regulates the phosphorylated CREB in APP/PS1 Tg mice

Deficits in CREB signaling may be implicated in AD pathology through the detrimental effects of A [53, 54]. However, activation of CREB pathway induces anti-inflammatory effects and ameliorated cognitive deficits [55]. Therefore, we tested the p-CREB protein level to clarify whether or not CREB, the H3R downstream signaling, is involved in the thioperamide mediated glial inactivation and anti-inflammatory

effect in AD. In consistent with the previous reports, decreased intensity of p-CREB immunostaining was observed either in hippocampus (reduced to 67.05 ± 6.424% of WT, $P$ <0.05, Fig. 5A, B) or in cortex (reduced to 51.07 ± 1.184% of WT, $P$ <0.001, Fig. 5A, C) of APP/PS1 Tg mice compared to the WT mice. As expect, thioperamide up-regulated the p-CREB intensity remarkably (increased to 96.52 ± 5.964% of WT, $P$ <0.05, Fig. 5A, B; increased to 86.70 ± 2.965% of WT, $P$ <0.001, Fig. 5A, C) in APP/PS1 Tg mice. In addition, results of western blot also suggested that the expression of phosphorylated CREB decreased significantly (decreased to 60.52 ± 4.572% of WT, $P$ <0.01, Fig. 5D, E) in hippocampus of APP/PS1 Tg mice, which was reversed markedly by thioperamide (increased to 86.70 ± 2.965% of WT, $P$ <0.01, Fig. 5D, E).

It has been well known that the expression of pro-inflammatory cytokines requires NF-κB activation. Therefore, we investigated the effect of thioperamide on the activation of NF-κB. Interestingly, the results indicated that the expression of phosphorylated NF-κB p65 increased significantly (increased to 325.8 ± 48.64% of WT, $P$ <0.01, Fig. 5D, F) in hippocampus of APP/PS1 Tg mice compared with the WT mice, which was compromised by administration of thioperamide (decreased to 160.1 ± 31.17% of WT, $P$ <0.05, Fig. 5D, F). Together, all these results showed that AD induced a decreased expression of p-CREB, whereas up-regulated p-NF-κB p65 and treatment with thioperamide significantly activated the CREB signaling and suppressed the activation of NF-κB p65.

## Activation of CREB is involved in the effects of thioperamide on glial reactivity and inflammatory response in APP/PS1 Tg mice

In order to further investigate the involvement of CREB signaling in the effects of thioperamide on the activation of microglia and astrocytes, H89, the inhibitor of PKA/CREB was administrated to inhibit p-CREB. The results showed that the area of $Iba1^+$-cells in both hippocampus and cortex markedly increased in the thioperamide + H89 group compared with the thioperamide group in APP/PS1 Tg mice (from 2.370 ± 0.2887 to 4.534 ± 0.2449 in hippocampus, $P$ <0.05; from 1.721 ± 0.06341 to 3.333 ± 0.2425 in hippocampus, $P$ <0.01, Fig. 6A, C). Similarly, the inhibitory effect of thioperamide on reactivated astrocytes area was also reversed by administration of H89 in either hippocampus or cortex in APP/PS1 Tg mice (from 1.183 ± 0.2078 to 2.806 ± 0.4070 in hippocampus, $P$ <0.01; from 0.7970 ± 0.1013 to 2.1060 ± 0.2257 in cortex, $P$ <0.05, Fig. 6A, C). Above all, results suggested that activation of CREB was involved in the alleviated reactive glial cells offered by thioperamide in AD.

Furthermore, we examined the role of CREB activation in the anti-inflammation offered by thioperamide. As expect, levels of IL-1β (from 410.1 ± 23.45 to 535.8 ± 42.90 in hippocampus, $P$ <0.05; from 417.5 ± 27.05 to 562.9 ± 43.9 in cortex, $P$ <0.05, Fig. 6E) and TNFα (from 695.2 ± 45.03 to 902.6 ± 39.53 in hippocampus, $P$ <0.01; from 715.0 ± 45.66 to 916.3 ± 31.33 in cortex, $P$ <0.01, Fig. 6F) increased markedly in the thioperamide+H89 group compared with the thioperamide group in APP/PS1 Tg mice. In addition, the up-regulated anti-inflammatory cytokine IL-4 was obviously reversed by administration of H89 in APP/PS1 Tg mice (from 514.0 ± 30.08 to 344.5 ± 35.03 in hippocampus, $P$ <0.01; from 509.9 ±

25.91 to 350.0 ± 30.00 in cortex, $P$ <0.01, Fig. 6G). Results above showed that activation of CREB was also involved in the anti-inflammatory effects offered by thioperamide in AD.

### Thioperamide reduces Aβ burden through CREB activation in APP/PS1 Tg mice

The reactive glial cells in AD induce enhanced inflammatory cytokines release, which contributes to the accumulation of pathologic Aβ [12]. Therefore, we further examined the plaque deposition and soluble Aβ levels to investigate whether the up-regulated p-CREB by thioperamide was involved in the Aβ pathology. We observed a dramatic reduction in plaque burden in the hippocampus and cortex with thioflavin-S staining in the thioperamide group compared with the vehicle group in APP/PS1 Tg mice, which was obviously reversed by administration of H89 (Fig. 3A, B). The quantitative analysis indicated that thioperamide down-regulated the area of Aβ-positive plaque burden in both hippocampus and cortex significantly (from 7.805 ± 0.8837% to 3.729 ± 0.2948% in hippocampus, $P$ <0.01, Fig. 7C; from 10.33 ± 0.7218% to 4.584 ± 0.4692% in cortex, $P$ <0.01, Fig. 7D). H89 treatment reversed the decreased Aβ-positive plaque by thioperamide markedly (increased to 7.339 ± 0.8506% in hippocampus, $P$ <0.05, Fig. 7C; increased to 8.726 ± 1.227% in cortex, $P$ <0.05, Fig. 7D).

Moreover, we also assessed the levels of $A\beta_{40}$ and $A\beta_{42}$ by using a quantitative ELISA. The ELISA results showed that the soluble $A\beta_{40}$ (from 891.2 ± 39.85 to 643.3 ± 51.46 in hippocampus, $P$ <0.01, Fig. 7E; from 1327 ± 67.54 to 918.5 ± 66.4 in cortex, $P$ <0.01, Fig. 7F) and $A\beta_{42}$ (from 671.4 ± 29.15 to 407.0 ± 29.74 in hippocampus, $P$ <0.001, Fig. 7G; from 756.0 ± 41.81 to 531.3 ± 59.57 in cortex, $P$ <0.05, Fig. 7H) levels in both hippocampus and cortex in thioperamide group were significantly lower than those in vehicle group in APP/PS1 Tg mice. Treatment with H89 obviously reversed the lowered levels of both $A\beta_{40}$ (increased to 849.1 ± 33.62 in hippocampus, $P$ <0.05, Fig. 7E; increased to 1246 ± 74.53 in cortex, $P$ <0.05, Fig. 7F) and $A\beta_{42}$ (increased to 584.2 ± 48.58 in hippocampus, $P$ <0.05, Fig. 7G; increased to 740.2 ± 38.41 in cortex, $P$ <0.05, Fig. 7H). The above data clearly demonstrated that thioperamide decreased Aβ burden in APP/PS1 mice via activating CREB pathway.

### Thioperamide attenuates cognitive impairments through CREB activation in APP/PS1 Tg mice

Furthermore, the effect of thioperamide and H89 on behavior was also tested to elucidate the effect of thioperamide on cognition and related mechanism in APP/PS1 Tg mice. The novel object recognition (NOR) test indicated that time spending on novel objection decreased significantly in the APP/PS1 group compared with the WT group (from 68.25 ± 5.008% to 48.54 ± 2.284%, $P$ <0.01, Fig. 8A). Administration of thioperamide significantly increased the time spending on novel object by (to 65.08 ± 3.910%, $P$ <0.05, Fig. 8A), which was reversed significantly by H89 treatment (to 48.88 ± 3.031%, $P$ <0.05, Fig. 8A). In the Y maze (YM) test, we observed a decreased SA% (spontaneous alternation %) in the APP/PS1 group compared with the WT group (from 82.58 ± 3.64% to 54.40 ± 6.397%, $P$ <0.01, Fig. 8B). Administration of thioperamide increased the SA% to 78.77 ± 4.975% significantly in APP/PS1 Tg mice ($P$ <0.01, Fig. 8B), which was reversed by H89 treatment to 52.56 ± 4.177% significantly ($P$ <0.01, Fig. 8B). In morris water maze (MWM) test, the escape latency increased significantly in the APP/PS1 group on day 3 to day 5 ($P$

<0.001, Fig. 8C). Administration of thioperamide significantly decreased the escape latency ($P$ <0.001, Fig. 8C), which was reversed markedly by H89 treatment ($P$ <0.05, Fig. 8C). Moreover, times crossing the platform decreased in APP/PS1 Tg mice (from 6.625 ± 0.9051 to 1.750 ± 0.491, $P$ <0.001, Fig. 8D) on day 6, and administration of thioperamide increased it significantly (to 5.875 ± 0.8332, $P$ <0.01, Fig. 8D). H89 treatment reversed the effect of thioperamide obviously to 2.750 ± 0.4532 ($P$ <0.05, Fig. 8D). Results above suggested that thioperamide improved the cognitive impairments through activation of CREB signaling pathway in APP/PS1 Tg mice.

# Discussion

In this study, we have shown that inhibition of H3R by thioperamide could modulate the gliosis and confers protection from pathological hallmarks and cognitive impairment in a mouse model of AD. Specifically, we found that thioperamide induced a lower reactivity of glial cells around Aβ plaques, attenuated neuroinflammation, reduced soluble Aβ, and ultimately resulting in a better cognitive outcome. Importantly, the effect of thioperamide on reactivity of glial cells, neuroinflammation, Aβ deposition and cognitive function in AD were compromised by treatment with H89, a PKA/CREB inhibitor, suggesting a CREB dependent mechanism.

Up to now, no therapy is available to block or slow down AD progression, and the mechanisms of AD are not fully understood [56]. Proliferation and activation of microglia concentrated around amyloid plaques, is a prominent feature of AD, which plays a key role in the pathogenesis of AD [57]. In AD pathogenesis, microglia activation plays a dual role: on one side, acute microglial activation in some experimental paradigms leads to decreased Aβ accumulation by increasing phagocytosis or clearance. In contrast, chronic activation of microglia contributes to neurotoxicity and synapse loss by triggering several proinflammatory cascades [58].

It is reported that whilst H3R are preserved in AD brain, higher density of H3R correlated with more severe dementia [29, 59, 60]. H3R agonist (R)-α-methylhistamine (RAMH) induces impaired learning and memory [59], while H3R knockout enhanced cognitive function [61, 62]. Recent reports show that H3R are highly expressed not only in neurons but also in microglia and astrocytes to regulate the inflammatory response [63, 64]. However, the role of H3R in modulation of reactivity of gliosis in AD has not been reported. To further explore the effect of thioperamide on microgliosis in AD, experiments were carried out by using APP/PS1 Tg mice. Our results showed that APP/PS1 Tg mice induce an obvious activation of microglia, which was reversed by thioperamide treatment. Therefore, this study suggested that inhibition of H3R by thioperamide could inhibit the microgliosis in AD.

In addition to neurotoxicity, activated microglia can enhance the activation of adjacent astrocytes by releasing factors such TNFα and IL-1β that can further magnify neuronal injury [65]. Reactive astrocytes have traditionally been considered a uniform response mechanism of the brain to acute or chronic injury. However, recent studies have demonstrated that reactive astrocytes could create either detrimental or beneficial conditions for damaged neurons, likely depending on the nature, severity, and duration of the

pathological stimulus [66]. Neuroinflammation in AD could induce two different types of reactive astrocytes that we termed protective “A2” and neurotoxic “A1” [66, 67]. Moreover, the abovementioned studies have provided evidence that many neurotoxic pathways are directly executed by astrocytes, with microglia perhaps playing a triggering or initiating role [65, 66]. Interestingly, we found that thioperamide induced a lower reactivity of astrocytes in either hippocampus or cortex in APP/PS1 Tg mice. More importantly, a reduced expression of C3, a characteristic product of “A1” astrocytes [66] that contributes to AD pathology [68], while increased expression of S100A10, a characteristic product of “A2” astrocytes [69] that confers protection against AD pathology [66] were observed with treatment of thioperamide, indicating that inhibition of H3R contributes to a shift from toxic to protective astrocyte phenotypes in AD mice. Reactive astrocytes recruited to the Aβ plaques likely prolong the neuroinflammatory process by secreting proinflammatory molecules, such as IL-1β and TNF-α, which might lead to pathogenic chronic neuroinflammation and contribute to progression of pathology in AD [50, 70, 71]. As expect, we also found a lower reactivity of astrocytes around Aβ plaques. As an autoreceptor, H3R could enhance the release of histamine in a feedback way. Consistent with our results, histamine also attenuates astrogliosis in spinal cord injury [72] and cerebral ischemic injury [73], suggesting a modulation of astrocytic function by histaminergic system. Our results demonstrated for the first time that inhibition of histamine H3R could suppress the activation of astrocytes and promote shift from toxic A1 to protective A2 astrocyte phenotypes in AD.

Deposition of Aβ triggers microgliosis and astrogliosis, both of which contribute to the pathogenesis of AD [7]. Gliosis is responsible for the secretion of pro- and anti-inflammatory cytokines (e.g. TNF-α, IL-1β, IL-4) [74]. More importantly, chronic neuroinflammation, manifested as gliosis and production of pro-inflammatory cytokines, is an invariant hallmark of AD [7], indicating that an inflammatory response further promoted the injury of the brain in AD. Another result reveals that H3R antagonist GSK247246 could inhibit gliosis and induces anti- neuroinflammatory effect under white matter injury in the brain [75]. Consistent with the results, here we demonstrated that except for activation of glial cells, enhanced levels of IL-1β and TNF-α and decreased level of IL-4 were also observed in AD. H3R inhibition by thioperamide suppressed inflammatory response in AD, as it was demonstrated by down-regulated levels of pro-inflammatory cytokines IL-1β and TNF-α, and up-regulated level of anti-inflammatory cytokine IL-4. Conversely, there is report shows that activation but not inhibition of microglial H3R suppresses LPS-induced proinflammatory activities [63]. Concerning that acute moderate activation of microglia promotes anti-inflammation M2 microglia phenotypes, whereas chronic microglial activation exerts pro-inflammation M1 phenotypes in AD [76]. The differences might be attributed to the regulation of two different polarization of microglia by different factors.

To further understand the molecular mechanism underlying the effect of thioperamide, we examined the protein expressions of p-CREB and p-P65NF-κB. Reduced p-CREB level has been observed in AD mice overexpressing Aβ [53]. Therefore, deficit in CREB signaling may be implicated in AD pathology through the detrimental effects of Aβ [35, 54, 77]. In addition, the decreased p-CREB expression is involved in the activation of glial cells and neuroinflammation in CNS [78-80]. CREB is also thought to be important for regulation of the inflammatory cytokines expression, and its dysfunction contributes to the pathogenesis

of AD [37], implicating CREB might play an important role in mediating the effect of thioperamide on inflammation in AD. Moreover, stimulates of CREB pathway also enhances the microglial M2 polarization [81], and inhibits glia-mediated inflammation [39, 82]. It is well acknowledged that inhibition of H3R induces CREB pathway activation [28]. Therefore, we investigated the effect of thioperamide on CREB phosphorylation in AD. As expect, a decreased level of p-CREB was observed in APP/PS1 Tg mice, and it was reversed by thioperamide treatment. H89, an inhibitor of protein kinase A (PKA)/CREB, compromised the alleviated effect of thioperamide on glial reactivity in AD, suggesting that thioperamide inhibited the activity of microglia and astrocytes in AD through activating CREB pathway. Both elevated anti-inflammatory factors and decreased inflammatory factors by thioperamide were also reversed by administration of H89, indicating that thioperamide inhibited the inflammatory response through activating CREB signaling.

Expression of pro-inflammatory cytokines requires NF-κB activation and its nuclear translocation to interact with DNA [83]. Study indicates that activation of CREB induces reduced expression of p-NF-κB and decreased production of proinflammatory cytokines in brain injury [84]. We found a significant increase of p-P65 NF-κB phosphorylation in APP/PS1 Tg mice, suggesting that Aβ could activate NF-κB signaling pathway. However, thioperamide treatment suppressed the levels of p-P65 NF-κB in APP/PS1 Tg mice. These data indicated that the anti-inflammatory effects of thioperamide might be mediated by inhibition of NF-κB activity.

Glial cells have a variety of functions in the brain, ranging from immune defense against external and endogenous hazardous stimuli, regulation of synaptic formation, calcium homeostasis, and metabolic support for neurons. Their dysregulation contributes to the cognitive decline and pathological development of AD. One of the most important functions of glial cells in AD is the regulation of Aβ levels in the brain [85]. Microglia and astrocytes have been reported to play a central role as moderators of Aβ clearance and degradation [86, 87]. Inflammation could reduce microglial clearance of Aβ in APP/PS1 Tg mice [88]. Inhibition of activated microglia and astrocytes could suppress the inflammatory response and attenuate the accumulation of Aβ, and ultimately protect mice against synaptic dysfunction and a decline in spatial cognition [89]. Therefore, we further studied the effect of thioperamide on Aβ clearance and related mechanism. Interestingly, we found that thioperamide treatment decreased the level of Aβ either in hippocampus or cortex. More importantly, H89 reversed the effect of thioperamide on Aβ clearance, indicating a CREB dependent mechanism. Furthermore, we also valuated cognitive function based on the NOR test, Y maze test and MWM test. Our results showed that APP/PS1 Tg mice showed memory impairment and could be rescued by thioperamide administration. H89 treatment reversed the ameliorated cognition offered by thioperamide, suggesting CREB pathway was involved in the alleviated effect of thioperamide on cognitive dysfunction.

# Conclusions

The present study indicates that H3R antagonist thioperamide improved cognitive impairment in APP/PS1 Tg mice via modulation of the CREB-mediated inhibited gliosis and inflammation, which

contributed to Aβ clearance. These results uncovered a novel mechanism behind the therapeutic effect of thioperamide in AD and further provided an experimental basis for starting a clinical trial for H3R antagonists as a treatment for AD.

# Abbreviations

AD: Alzheimer's disease; H3R: Histamine H3 receptor; Aβ: β-Amyloid; Iba1: Ionized calcium binding adapter molecule 1; GFAP: Glial fibrillary acidic protein; C3: Complement 3; S100A10: S100 calcium binding protein A10; APP/PS1 Tg mice: APPswe/PSEN1dE9 transgenic mice; APP: Amyloid precursor protein; PS1: Presenilin-1; TNFα: Tumor necrosis factor α; IL-1β: Interleukin-1β; IL-4: Interleukin-4; CREB: Cyclic AMP response element-binding protein; NF-kB: Nuclear factor kappa-B; ELISA: Enzyme-linked immunosorbent assay; NOR: novel object recognition; YM: Y maze; MWM: Morris water maze; GRCR: G -protein-coupled receptor; PBS: phosphate buffer saline; BSA: Bovine serum albumin; SA%: alternation percentage; ANOVA: Analysis of variance; Thio: Thioperamide

# Declarations


### Acknowledgements

The authors would like to acknowledge Xuezhen Wang for her generous assistance in the lab.

### Funding

This study was supported by National Natural Science Foundation of China (81500930, 81901380), and Natural Science Foundation of Shandong Province (ZR2014HQ014, ZR2017BC047).


### Availability of data and materials

The datasets used and/or analyzed during the current study are available from the corresponding author on reasonable request.

### Authors' contributions

HY conceived and designed the project. HY, JW, BL, YX, CW, M.Y, C.Y.W., MS, JL, JY, FS, and WW performed the experiments. HY, JW, and BL analyzed the data and drafted the manuscript. All authors reviewed the manuscript. All authors read and approved the final manuscript.

### Ethics approval and consent to participate

Not applicable

### Consent for publication

Not applicable

### Competing interests

The authors declare no competing interests.

### Author details

[1]Department of Pharmacology, College of Basic Medicine, Binzhou Medical University, Yantai, China

[2]Institute for Metabolic and Neuropsychiatric Disorders, Binzhou Medical University Hospital, Binzhou, China

[3]Department of Thyroid Breast Surgery, Dongying People's Hospital, Dongying, China

## References

1. Crews L, Masliah E. Molecular mechanisms of neurodegeneration in Alzheimer's disease. Hum Mol Genet. 2010; 19:R12-20.
2. Long JM, Holtzman DM. Alzheimer Disease: An Update on Pathobiology and Treatment Strategies. Cell. 2019; 179:312-39.
3. Yankner BA, Lu T. Amyloid beta-protein toxicity and the pathogenesis of Alzheimer disease. J Biol Chem. 2009; 284:4755-9.
4. Keskin AD, Kekus M, Adelsberger H, Neumann U, Shimshek DR, Song B, Zott B, Peng T, Forstl H, Staufenbiel M, et al. BACE inhibition-dependent repair of Alzheimer's pathophysiology. Proc Natl Acad Sci U S A. 2017.
5. Hardy J, Selkoe DJ. The amyloid hypothesis of Alzheimer's disease: progress and problems on the road to therapeutics. Science. 2002; 297:353-6.
6. Piirainen S, Youssef A, Song C, Kalueff AV, Landreth GE, Malm T, Tian L. Psychosocial stress on neuroinflammation and cognitive dysfunctions in Alzheimer's disease: the emerging role for microglia? Neurosci Biobehav Rev. 2017; 77:148-64.
7. Ou Z, Kong X, Sun X, He X, Zhang L, Gong Z, Huang J, Xu B, Long D, Li J, et al. Metformin treatment prevents amyloid plaque deposition and memory impairment in APP/PS1 mice. Brain Behav Immun. 2018; 69:351-63.
8. Yamamoto M, Kiyota T, Horiba M, Buescher JL, Walsh SM, Gendelman HE, Ikezu T. Interferon-gamma and tumor necrosis factor-alpha regulate amyloid-beta plaque deposition and beta-secretase expression in Swedish mutant APP transgenic mice. Am J Pathol. 2007; 170:680-92.
9. Morihara T, Teter B, Yang F, Lim GP, Boudinot S, Boudinot FD, Frautschy SA, Cole GM. Ibuprofen suppresses interleukin-1beta induction of pro-amyloidogenic alpha1-antichymotrypsin to ameliorate beta-amyloid (Abeta) pathology in Alzheimer's models. Neuropsychopharmacology. 2005; 30:1111-20.

10. Cho MH, Cho K, Kang HJ, Jeon EY, Kim HS, Kwon HJ, Kim HM, Kim DH, Yoon SY. Autophagy in microglia degrades extracellular beta-amyloid fibrils and regulates the NLRP3 inflammasome. Autophagy. 2014; 10:1761-75.
11. Cai Q, Li Y, Pei G. Polysaccharides from Ganoderma lucidum attenuate microglia-mediated neuroinflammation and modulate microglial phagocytosis and behavioural response. J Neuroinflammation. 2017; 14:63.
12. Heneka MT, Carson MJ, El Khoury J, Landreth GE, Brosseron F, Feinstein DL, Jacobs AH, Wyss-Coray T, Vitorica J, Ransohoff RM, et al. Neuroinflammation in Alzheimer's disease. Lancet Neurol. 2015; 14:388-405.
13. Rossi D. Astrocyte physiopathology: At the crossroads of intercellular networking, inflammation and cell death. Prog Neurobiol. 2015; 130:86-120.
14. Akiyama H, Barger S, Barnum S, Bradt B, Bauer J, Cole GM, Cooper NR, Eikelenboom P, Emmerling M, Fiebich BL, et al. Inflammation and Alzheimer's disease. Neurobiol Aging. 2000; 21:383-421.
15. Wyss-Coray T. Inflammation in Alzheimer disease: driving force, bystander or beneficial response? Nat Med. 2006; 12:1005-15.
16. Wada H, Inagaki N, Yamatodani A, Watanabe T. Is the histaminergic neuron system a regulatory center for whole-brain activity? Trends Neurosci. 1991; 14:415-8.
17. Haas H, Panula P. The role of histamine and the tuberomamillary nucleus in the nervous system. Nat Rev Neurosci. 2003; 4:121-30.
18. Haas HL, Sergeeva OA, Selbach O. Histamine in the nervous system. Physiol Rev. 2008; 88:1183-241.
19. Brown RE, Stevens DR, Haas HL. The physiology of brain histamine. Prog Neurobiol. 2001; 63:637-72.
20. Arrang JM, Garbarg M, Schwartz JC. Auto-inhibition of brain histamine release mediated by a novel class (H3) of histamine receptor. Nature. 1983; 302:832-7.
21. Morisset S, Rouleau A, Ligneau X, Gbahou F, Tardivel-Lacombe J, Stark H, Schunack W, Ganellin CR, Schwartz JC, Arrang JM. High constitutive activity of native H3 receptors regulates histamine neurons in brain. Nature. 2000; 408:860-4.
22. Schlicker E, Betz R, Gothert M. Histamine H3 receptor-mediated inhibition of serotonin release in the rat brain cortex. Naunyn Schmiedebergs Arch Pharmacol. 1988; 337:588-90.
23. Schlicker E, Fink K, Hinterthaner M, Gothert M. Inhibition of noradrenaline release in the rat brain cortex via presynaptic H3 receptors. Naunyn Schmiedebergs Arch Pharmacol. 1989; 340:633-8.
24. Schlicker E, Fink K, Detzner M, Gothert M. Histamine inhibits dopamine release in the mouse striatum via presynaptic H3 receptors. J Neural Transm Gen Sect. 1993; 93:1-10.
25. Dai H, Fu Q, Shen Y, Hu W, Zhang Z, Timmerman H, Leurs R, Chen Z. The histamine H3 receptor antagonist clobenpropit enhances GABA release to protect against NMDA-induced excitotoxicity through the cAMP/protein kinase A pathway in cultured cortical neurons. Eur J Pharmacol. 2007; 563:117-23.

26. Hansen KB, Mullasseril P, Dawit S, Kurtkaya NL, Yuan H, Vance KM, Orr AG, Kvist T, Ogden KK, Le P, et al. Implementation of a fluorescence-based screening assay identifies histamine H3 receptor antagonists clobenpropit and iodophenpropit as subunit-selective N-methyl-D-aspartate receptor antagonists. J Pharmacol Exp Ther. 2010; 333:650-62.
27. Clapham J, Kilpatrick GJ. Histamine H3 receptors modulate the release of [3H]-acetylcholine from slices of rat entorhinal cortex: evidence for the possible existence of H3 receptor subtypes. Br J Pharmacol. 1992; 107:919-23.
28. Leurs R, Bakker RA, Timmerman H, de Esch IJ. The histamine H3 receptor: from gene cloning to H3 receptor drugs. Nat Rev Drug Discov. 2005; 4:107-20.
29. Medhurst AD, Atkins AR, Beresford IJ, Brackenborough K, Briggs MA, Calver AR, Cilia J, Cluderay JE, Crook B, Davis JB, et al. GSK189254, a novel H3 receptor antagonist that binds to histamine H3 receptors in Alzheimer's disease brain and improves cognitive performance in preclinical models. J Pharmacol Exp Ther. 2007; 321:1032-45.
30. Brioni JD, Esbenshade TA, Garrison TR, Bitner SR, Cowart MD. Discovery of histamine H3 antagonists for the treatment of cognitive disorders and Alzheimer's disease. J Pharmacol Exp Ther. 2011; 336:38-46.
31. Bitner RS, Markosyan S, Nikkel AL, Brioni JD. In-vivo histamine H3 receptor antagonism activates cellular signaling suggestive of symptomatic and disease modifying efficacy in Alzheimer's disease. Neuropharmacology. 2011; 60:460-6.
32. Patnaik R, Sharma A, Skaper SD, Muresanu DF, Lafuente JV, Castellani RJ, Nozari A, Sharma HS. Histamine H3 Inverse Agonist BF 2649 or Antagonist with Partial H4 Agonist Activity Clobenpropit Reduces Amyloid Beta Peptide-Induced Brain Pathology in Alzheimer's Disease. Mol Neurobiol. 2018; 55:312-21.
33. Eissa N, Jayaprakash P, Azimullah S, Ojha SK, Al-Houqani M, Jalal FY, Lazewska D, Kiec-Kononowicz K, Sadek B. The histamine H3R antagonist DL77 attenuates autistic behaviors in a prenatal valproic acid-induced mouse model of autism. Sci Rep. 2018; 8:13077.
34. Hiraga N, Adachi N, Liu K, Nagaro T, Arai T. Suppression of inflammatory cell recruitment by histamine receptor stimulation in ischemic rat brains. Eur J Pharmacol. 2007; 557:236-44.
35. Yin Y, Gao D, Wang Y, Wang ZH, Wang X, Ye J, Wu D, Fang L, Pi G, Yang Y, et al. Tau accumulation induces synaptic impairment and memory deficit by calcineurin-mediated inactivation of nuclear CaMKIV/CREB signaling. Proc Natl Acad Sci U S A. 2016; 113:E3773-81.
36. Wang Z, Zhang YH, Zhang W, Gao HL, Zhong ML, Huang TT, Guo RF, Liu NN, Li DD, Li Y, et al. Copper chelators promote nonamyloidogenic processing of AbetaPP via MT1/2 /CREB-dependent signaling pathways in AbetaPP/PS1 transgenic mice. J Pineal Res. 2018; 65:e12502.
37. Bartolotti N, Lazarov O. CREB signals as PBMC-based biomarkers of cognitive dysfunction: A novel perspective of the brain-immune axis. Brain Behav Immun. 2019; 78:9-20.
38. Qin X, Liu Y, Feng Y, Jiang J. Ginsenoside Rf alleviates dysmenorrhea and inflammation through the BDNF-TrkB-CREB pathway in a rat model of endometriosis. Food Funct. 2019; 10:244-9.

39. Alexaki VI, Fodelianaki G, Neuwirth A, Mund C, Kourgiantaki A, Ieronimaki E, Lyroni K, Troullinaki M, Fujii C, Kanczkowski W, et al. DHEA inhibits acute microglia-mediated inflammation through activation of the TrkA-Akt1/2-CREB-Jmjd3 pathway. Mol Psychiatry. 2018; 23:1410-20.
40. Wang B, Chen T, Wang J, Jia Y, Ren H, Wu F, Hu M, Chen Y. Methamphetamine modulates the production of interleukin-6 and tumor necrosis factor-alpha via the cAMP/PKA/CREB signaling pathway in lipopolysaccharide-activated microglia. Int Immunopharmacol. 2018; 56:168-78.
41. Guan X, Wang Y, Kai G, Zhao S, Huang T, Li Y, Xu Y, Zhang L, Pang T. Cerebrolysin Ameliorates Focal Cerebral Ischemia Injury Through Neuroinflammatory Inhibition via CREB/PGC-1alpha Pathway. Front Pharmacol. 2019; 10:1245.
42. Takahashi K, Nakagawasai O, Nemoto W, Kadota S, Isono J, Odaira T, Sakuma W, Arai Y, Tadano T, Tan-No K. Memantine ameliorates depressive-like behaviors by regulating hippocampal cell proliferation and neuroprotection in olfactory bulbectomized mice. Neuropharmacology. 2018; 137:141-55.
43. Liu B, Liu J, Wang JG, Liu CL, Yan HJ. AdipoRon improves cognitive dysfunction of Alzheimer's disease and rescues impaired neural stem cell proliferation through AdipoR1/AMPK pathway. Exp Neurol. 2020:113249.
44. Yan H, Zhang X, Hu W, Ma J, Hou W, Zhang X, Wang X, Gao J, Shen Y, Lv J, et al. Histamine H3 receptors aggravate cerebral ischaemic injury by histamine-independent mechanisms. Nat Commun. 2014; 5:3334.
45. Liu B, Liu J, Wang J, Sun F, Jiang S, Hu F, Wang D, Liu D, Liu C, Yan H. Adiponectin Protects Against Cerebral Ischemic Injury Through AdipoR1/AMPK Pathways. Front Pharmacol. 2019; 10:597.
46. Chiba T, Yamada M, Sasabe J, Terashita K, Shimoda M, Matsuoka M, Aiso S. Amyloid-beta causes memory impairment by disturbing the JAK2/STAT3 axis in hippocampal neurons. Mol Psychiatry. 2009; 14:206-22.
47. Vorhees CV, Williams MT. Morris water maze: procedures for assessing spatial and related forms of learning and memory. Nature Protocols. 2006; 1:848-58.
48. Okello A, Edison P, Archer HA, Turkheimer F, Kennedy J, Bullock R, Walker Z, Kennedy A, Fox N, Rossor M, Brooks D. Microglial activation and amyloid deposition in mild cognitive impairment: A PET study. Neurology. 2009; 72:56-62.
49. Osborn LM, Kamphuis W, Wadman WJ, Hol EM. Astrogliosis: An integral player in the pathogenesis of Alzheimer's disease. Progress in Neurobiology. 2016; 144:121-41.
50. Carter SF, Herholz K, Rosa-Neto P, Pellerin L, Nordberg A, Zimmer ER. Astrocyte Biomarkers in Alzheimer's Disease. Trends Mol Med. 2019; 25:77-95.
51. Liddelow SA, Guttenplan KA, Clarke LE, Bennett FC, Bohlen CJ, Schirmer L, Bennett ML, Munch AE, Chung WS, Peterson TC, et al. Neurotoxic reactive astrocytes are induced by activated microglia. Nature. 2017; 541:481-7.
52. Pekny M, Wilhelmsson U, Pekna M. The dual role of astrocyte activation and reactive gliosis. Neurosci Lett. 2014; 565:30-8.

53. Dineley KT, Westerman M, Bui D, Bell K, Ashe KH, Sweatt JD. Beta-amyloid activates the mitogen-activated protein kinase cascade via hippocampal alpha7 nicotinic acetylcholine receptors: In vitro and in vivo mechanisms related to Alzheimer's disease. J Neurosci. 2001; 21:4125-33.
54. Scott Bitner R. Cyclic AMP response element-binding protein (CREB) phosphorylation: a mechanistic marker in the development of memory enhancing Alzheimer's disease therapeutics. Biochem Pharmacol. 2012; 83:705-14.
55. Guo H, Cheng Y, Wang C, Wu J, Zou Z, Niu B, Yu H, Wang H, Xu J. FFPM, a PDE4 inhibitor, reverses learning and memory deficits in APP/PS1 transgenic mice via cAMP/PKA/CREB signaling and anti-inflammatory effects. Neuropharmacology. 2017; 116:260-9.
56. Di Meco A, Curtis ME, Lauretti E, Pratico D. Autophagy Dysfunction in Alzheimer's Disease: Mechanistic Insights and New Therapeutic Opportunities. Biol Psychiatry. 2020; 87:797-807.
57. Hansen DV, Hanson JE, Sheng M. Microglia in Alzheimer’s disease. Journal of Cell Biology. 2018; 217:459-72.
58. Sarlus H, Heneka MT. Microglia in Alzheimer's disease. J Clin Invest. 2017; 127:3240-9.
59. Sadek B, Saad A, Sadeq A, Jalal F, Stark H. Histamine H3 receptor as a potential target for cognitive symptoms in neuropsychiatric diseases. Behav Brain Res. 2016; 312:415-30.
60. Medhurst AD, Roberts JC, Lee J, Chen CP, Brown SH, Roman S, Lai MK. Characterization of histamine H3 receptors in Alzheimer's Disease brain and amyloid over-expressing TASTPM mice. Br J Pharmacol. 2009; 157:130-8.
61. Toyota H, Dugovic C, Koehl M, Laposky AD, Weber C, Ngo K, Wu Y, Lee DH, Yanai K, Sakurai E, et al. Behavioral characterization of mice lacking histamine H(3) receptors. Mol Pharmacol. 2002; 62:389-97.
62. Rizk A, Curley J, Robertson J, Raber J. Anxiety and cognition in histamine H3 receptor-/- mice. Eur J Neurosci. 2004; 19:1992-6.
63. Iida T, Yoshikawa T, Matsuzawa T, Naganuma F, Nakamura T, Miura Y, Mohsen AS, Harada R, Iwata R, Yanai K. Histamine H3 receptor in primary mouse microglia inhibits chemotaxis, phagocytosis, and cytokine secretion. Glia. 2015; 63:1213-25.
64. Juric DM, Krzan M, Lipnik-Stangelj M. Histamine and astrocyte function. Pharmacol Res. 2016; 111:774-83.
65. Kirkley KS, Popichak KA, Afzali MF, Legare ME, Tjalkens RB. Microglia amplify inflammatory activation of astrocytes in manganese neurotoxicity. J Neuroinflammation. 2017; 14:99.
66. Reichenbach N, Delekate A, Plescher M, Schmitt F, Krauss S, Blank N, Halle A, Petzold GC. Inhibition of Stat3-mediated astrogliosis ameliorates pathology in an Alzheimer's disease model. EMBO Mol Med. 2019; 11.
67. Xu X, Zhang A, Zhu Y, He W, Di W, Fang Y, Shi X. MFG-E8 reverses microglial-induced neurotoxic astrocyte (A1) via NF-kappaB and PI3K-Akt pathways. J Cell Physiol. 2018; 234:904-14.

68. Shi Q, Chowdhury S, Ma R, Le KX, Hong S, Caldarone BJ, Stevens B, Lemere CA. Complement C3 deficiency protects against neurodegeneration in aged plaque-rich APP/PS1 mice. Sci Transl Med. 2017; 9.
69. Fujita A, Yamaguchi H, Yamasaki R, Cui Y, Matsuoka Y, Yamada KI, Kira JI. Connexin 30 deficiency attenuates A2 astrocyte responses and induces severe neurodegeneration in a 1-methyl-4-phenyl-1,2,3,6-tetrahydropyridine hydrochloride Parkinson's disease animal model. J Neuroinflammation. 2018; 15:227.
70. Marutle A, Gillberg PG, Bergfors A, Yu W, Ni R, Nennesmo I, Voytenko L, Nordberg A. (3)H-deprenyl and (3)H-PIB autoradiography show different laminar distributions of astroglia and fibrillar beta-amyloid in Alzheimer brain. J Neuroinflammation. 2013; 10:90.
71. Avila-Munoz E, Arias C. When astrocytes become harmful: functional and inflammatory responses that contribute to Alzheimer's disease. Ageing Res Rev. 2014; 18:29-40.
72. Zhao YY, Yuan Y, Chen Y, Jiang L, Liao RJ, Wang L, Zhang XN, Ohtsu H, Hu WW, Chen Z. Histamine promotes locomotion recovery after spinal cord hemisection via inhibiting astrocytic scar formation. CNS Neurosci Ther. 2015; 21:454-62.
73. Liao RJ, Jiang L, Wang RR, Zhao HW, Chen Y, Li Y, Wang L, Jie LY, Zhou YD, Zhang XN, et al. Histidine provides long-term neuroprotection after cerebral ischemia through promoting astrocyte migration. Sci Rep. 2015; 5:15356.
74. Balducci C, Frasca A, Zotti M, La Vitola P, Mhillaj E, Grigoli E, Iacobellis M, Grandi F, Messa M, Colombo L, et al. Toll-like receptor 4-dependent glial cell activation mediates the impairment in memory establishment induced by beta-amyloid oligomers in an acute mouse model of Alzheimer's disease. Brain Behav Immun. 2017; 60:188-97.
75. Rangon CM, Schang AL, Van Steenwinckel J, Schwendimann L, Lebon S, Fu T, Chen L, Beneton V, Journiac N, Young-Ten P, et al. Myelination induction by a histamine H3 receptor antagonist in a mouse model of preterm white matter injury. Brain Behav Immun. 2018; 74:265-76.
76. Tang Y, Le W. Differential Roles of M1 and M2 Microglia in Neurodegenerative Diseases. Molecular Neurobiology. 2015; 53:1181-94.
77. Bartolotti N, Bennett DA, Lazarov O. Reduced pCREB in Alzheimer's disease prefrontal cortex is reflected in peripheral blood mononuclear cells. Mol Psychiatry. 2016; 21:1158-66.
78. Chen TT, Lan TH, Yang FY. Low-Intensity Pulsed Ultrasound Attenuates LPS-Induced Neuroinflammation and Memory Impairment by Modulation of TLR4/NF-kappaB Signaling and CREB/BDNF Expression. Cereb Cortex. 2019; 29:1430-8.
79. Hladik D, Dalke C, von Toerne C, Hauck SM, Azimzadeh O, Philipp J, Ung MC, Schlattl H, Rossler U, Graw J, et al. CREB Signaling Mediates Dose-Dependent Radiation Response in the Murine Hippocampus Two Years after Total Body Exposure. J Proteome Res. 2020; 19:337-45.
80. Hong ZY, Yu SS, Wang ZJ, Zhu YZ. SCM-198 Ameliorates Cognitive Deficits, Promotes Neuronal Survival and Enhances CREB/BDNF/TrkB Signaling without Affecting Abeta Burden in AbetaPP/PS1 Mice. Int J Mol Sci. 2015; 16:18544-63.

81. Luan B, Yoon YS, Le Lay J, Kaestner KH, Hedrick S, Montminy M. CREB pathway links PGE2 signaling with macrophage polarization. Proc Natl Acad Sci U S A. 2015; 112:15642-7.
82. Park T, Chen H, Kevala K, Lee JW, Kim HY. N-Docosahexaenoylethanolamine ameliorates LPS-induced neuroinflammation via cAMP/PKA-dependent signaling. J Neuroinflammation. 2016; 13:284.
83. Kaltschmidt B. NF-kB in the nervous system. Nuclear Factor Kb Regulation & Role in Disease. 2003.
84. Wu X, Fu S, Liu Y, Luo H, Li F, Wang Y, Gao M, Cheng Y, Xie Z. NDP-MSH binding melanocortin-1 receptor ameliorates neuroinflammation and BBB disruption through CREB/Nr4a1/NF-kappaB pathway after intracerebral hemorrhage in mice. J Neuroinflammation. 2019; 16:192.
85. Ries M, Sastre M. Mechanisms of Abeta Clearance and Degradation by Glial Cells. Front Aging Neurosci. 2016; 8:160.
86. Mandrekar S, Jiang Q, Lee CY, Koenigsknecht-Talboo J, Holtzman DM, Landreth GE. Microglia mediate the clearance of soluble Abeta through fluid phase macropinocytosis. J Neurosci. 2009; 29:4252-62.
87. Thal DR. The role of astrocytes in amyloid beta-protein toxicity and clearance. Exp Neurol. 2012; 236:1-5.
88. Tejera D, Mercan D, Sanchez-Caro JM, Hanan M, Greenberg D, Soreq H, Latz E, Golenbock D, Heneka MT. Systemic inflammation impairs microglial Abeta clearance through NLRP3 inflammasome. EMBO J. 2019; 38:e101064.
89. He XF, Liu DX, Zhang Q, Liang FY, Dai GY, Zeng JS, Pei Z, Xu GQ, Lan Y. Voluntary Exercise Promotes Glymphatic Clearance of Amyloid Beta and Reduces the Activation of Astrocytes and Microglia in Aged Mice. Front Mol Neurosci. 2017; 10:144.

# Figures

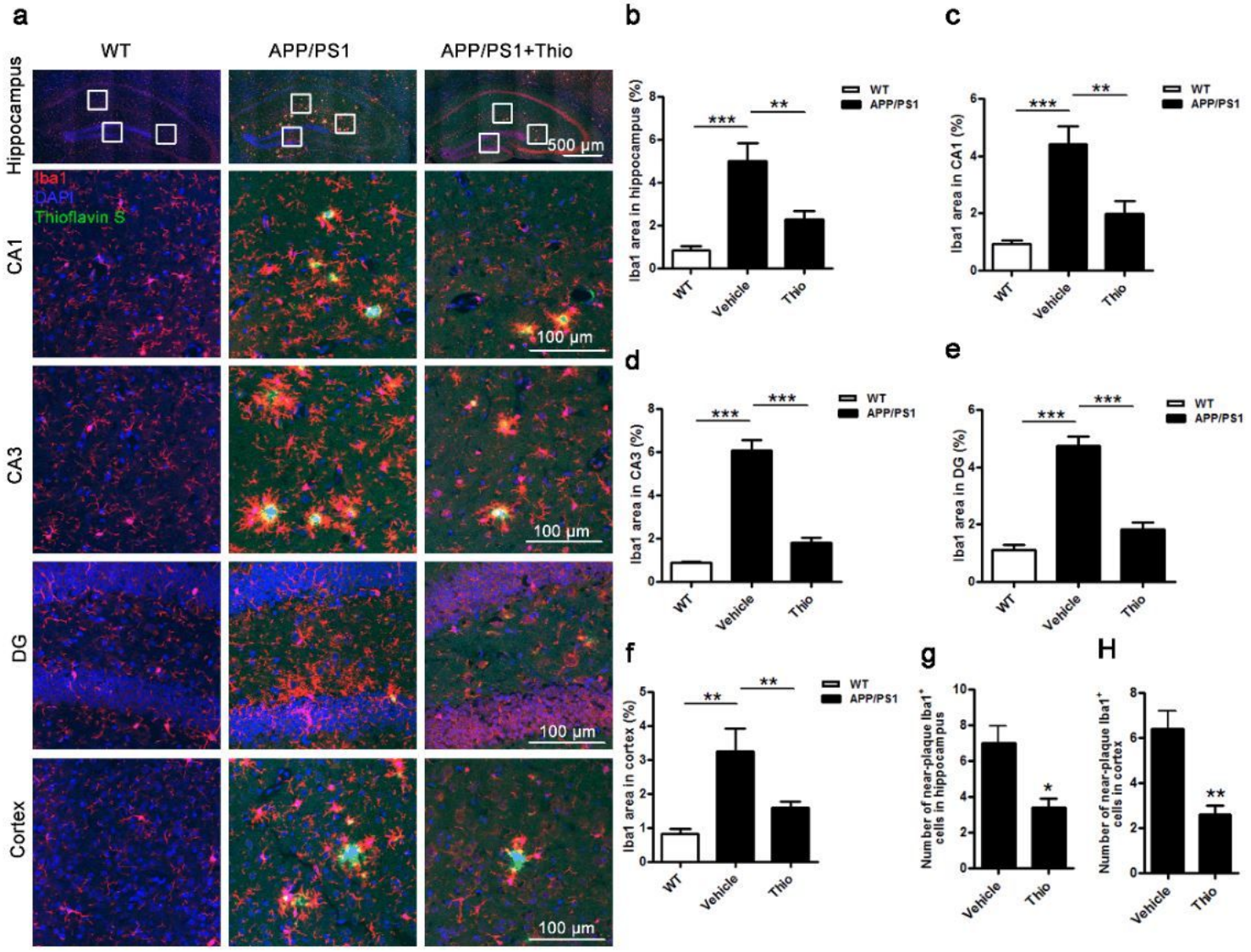


## Figure 1

Effect of thioperamide on microglial reactivity in APP/PS1 Tg mice. a-h Representative immunohistochemical staining of Iba1 (red) and bar graph in either hippocampus (a, b, g), including CA1 (a, c), CA3 (a, d) and DG (a, e) or cortex (a, f, h) showing the Iba1+ microglial reactivity (a-f) and numbers of near-plaque (≤ 50 μm, Thioflavin+) Iba1+ cells (a, g, h) in those receiving vehicle and thioperamide in WT and APP/PS1 Tg mice. Scale bar: 100 μm. n = 5 per group. *P <0.05, **P <0.01, ***P <0.001. Mean ± SEM. One-way ANOVA followed by Tukey's post hoc test.

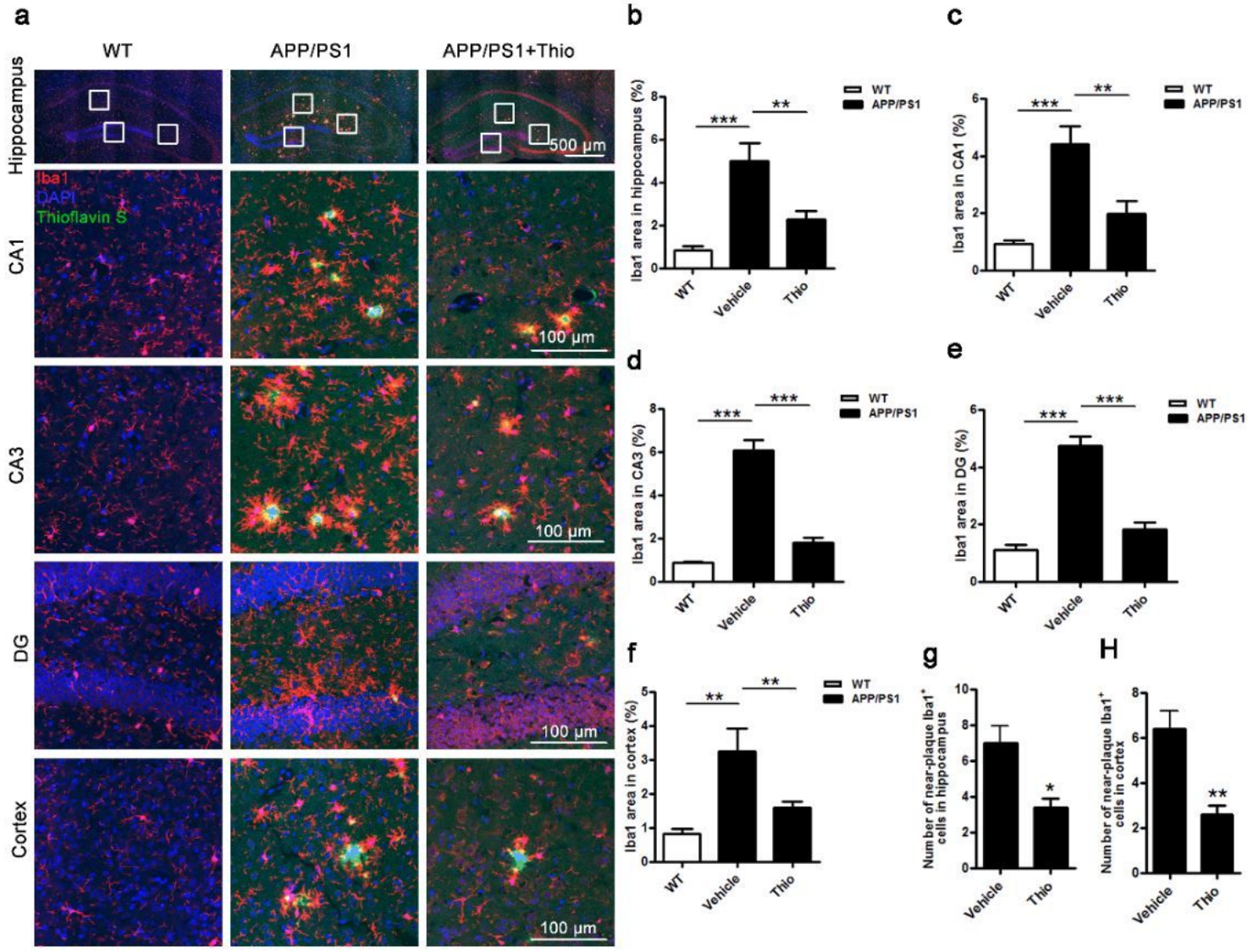


## Figure 1

Effect of thioperamide on microglial reactivity in APP/PS1 Tg mice. a-h Representative immunohistochemical staining of Iba1 (red) and bar graph in either hippocampus (a, b, g), including CA1 (a, c), CA3 (a, d) and DG (a, e) or cortex (a, f, h) showing the Iba1+ microglial reactivity (a-f) and numbers of near-plaque (≤ 50 μm, Thioflavin+) Iba1+ cells (a, g, h) in those receiving vehicle and thioperamide in WT and APP/PS1 Tg mice. Scale bar: 100 μm. n = 5 per group. *P <0.05, **P <0.01, ***P <0.001. Mean ± SEM. One-way ANOVA followed by Tukey's post hoc test.

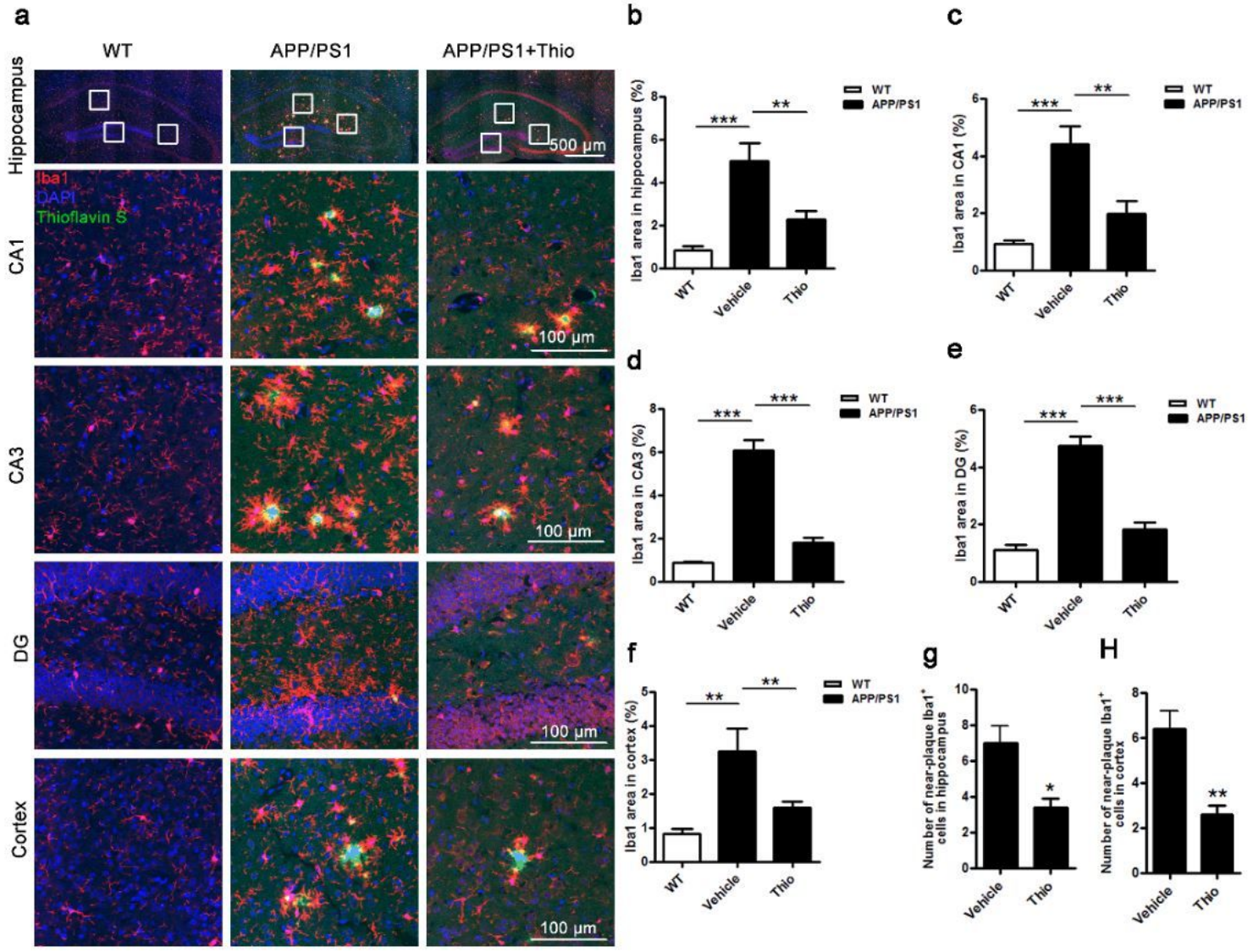


## Figure 1

Effect of thioperamide on microglial reactivity in APP/PS1 Tg mice. a-h Representative immunohistochemical staining of Iba1 (red) and bar graph in either hippocampus (a, b, g), including CA1 (a, c), CA3 (a, d) and DG (a, e) or cortex (a, f, h) showing the Iba1+ microglial reactivity (a-f) and numbers of near-plaque (≤ 50 μm, Thioflavin+) Iba1+ cells (a, g, h) in those receiving vehicle and thioperamide in WT and APP/PS1 Tg mice. Scale bar: 100 μm. n = 5 per group. *P <0.05, **P <0.01, ***P <0.001. Mean ± SEM. One-way ANOVA followed by Tukey's post hoc test.

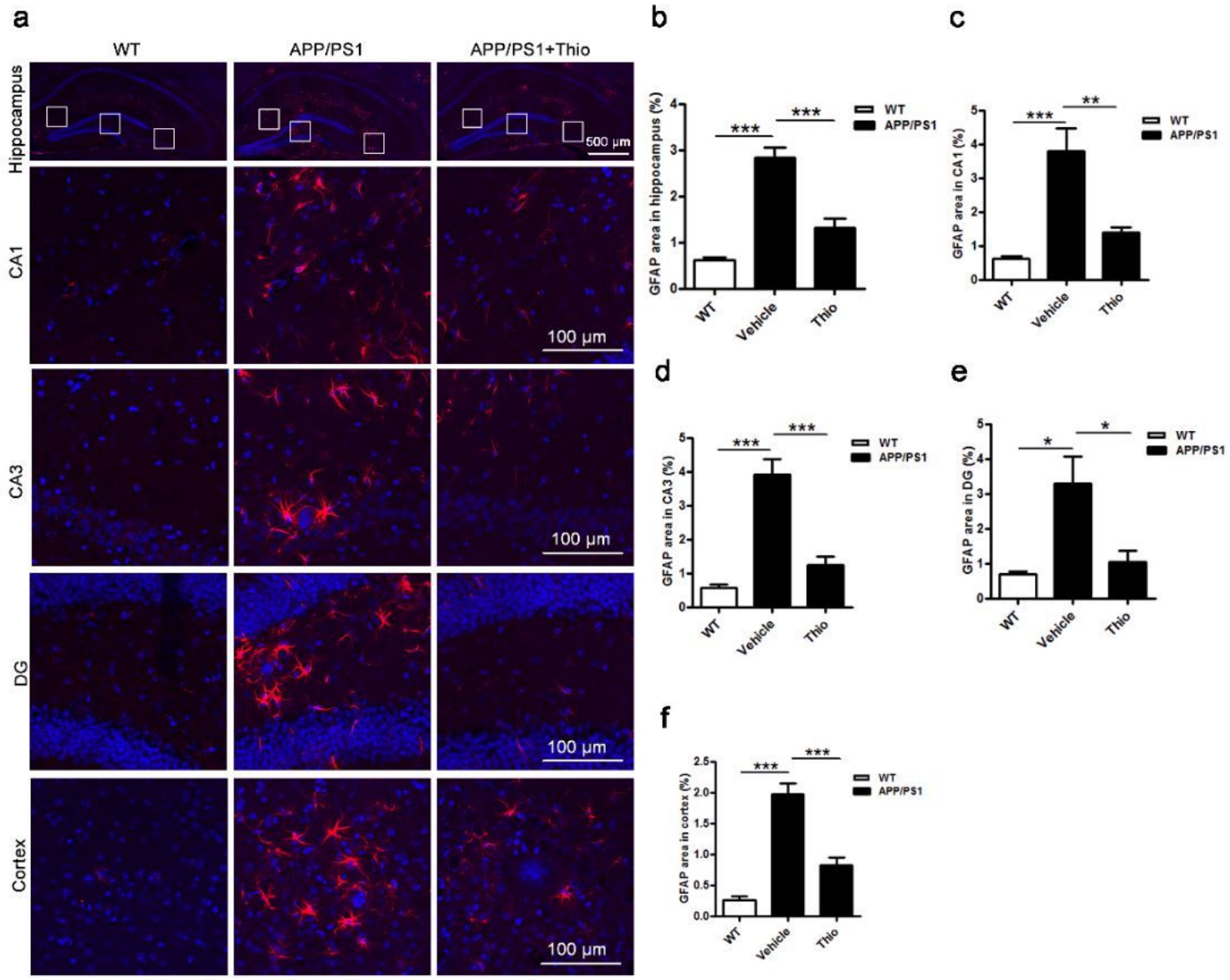


## Figure 2

Effect of thioperamide on astrocytic reactivity in APP/PS1 Tg mice. a-f Representative immunohistochemical staining of GFAP (red) and bar graph in either hippocampus (a, b), including CA1 (a, c), CA3 (a, d) and DG (a, e) or cortex (a, f) showing the GFAP+ astrocytic reactivity in those receiving vehicle and thioperamide in WT and APP/PS1 Tg mice. Scale bar: 100 μm. n = 5 per group. *P <0.05, **P <0.01, ***P <0.001. Mean ± SEM. One-way ANOVA followed by Tukey's post hoc test.

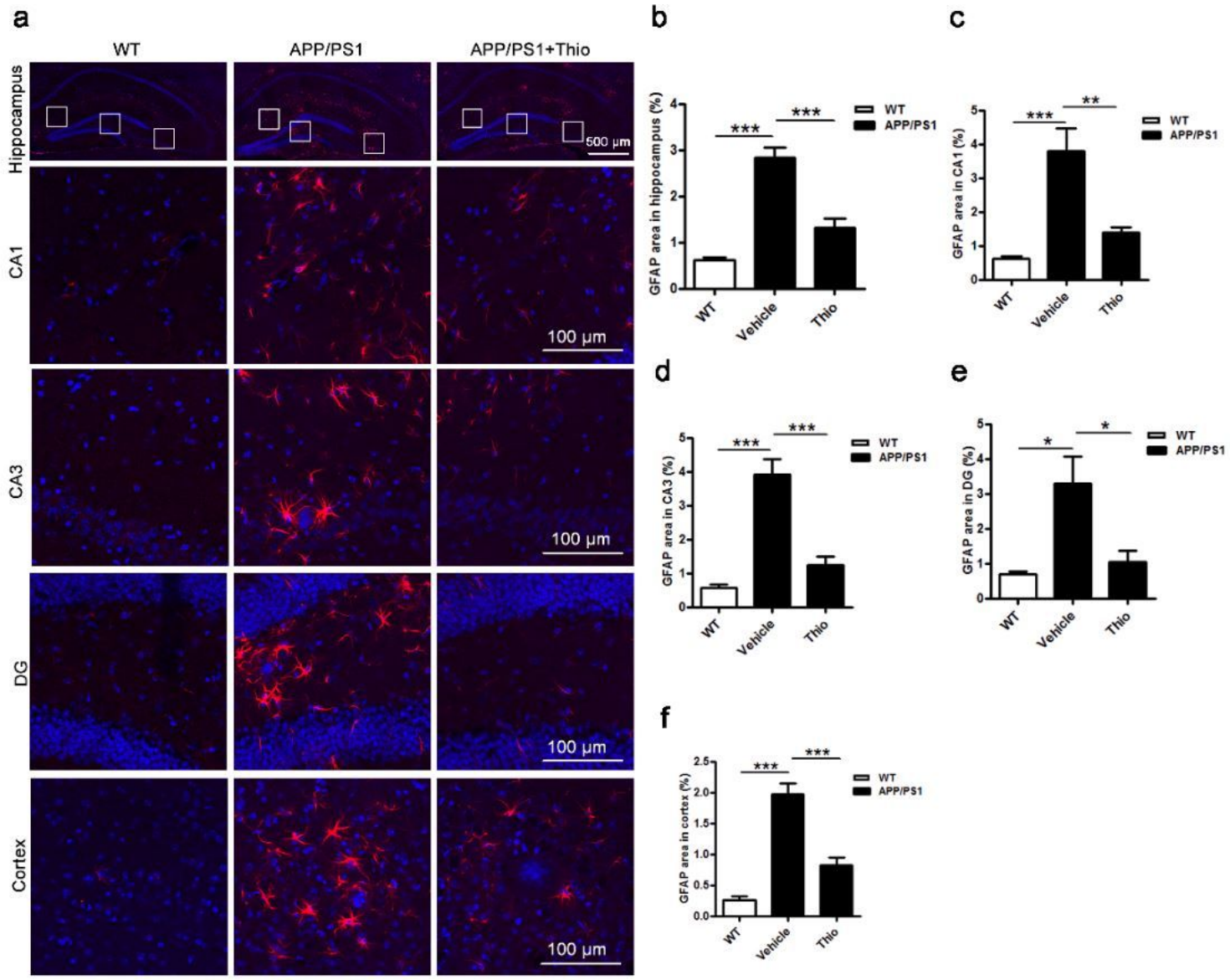


## Figure 2

Effect of thioperamide on astrocytic reactivity in APP/PS1 Tg mice. a-f Representative immunohistochemical staining of GFAP (red) and bar graph in either hippocampus (a, b), including CA1 (a, c), CA3 (a, d) and DG (a, e) or cortex (a, f) showing the GFAP+ astrocytic reactivity in those receiving vehicle and thioperamide in WT and APP/PS1 Tg mice. Scale bar: 100 μm. n = 5 per group. *P <0.05, **P <0.01, ***P <0.001. Mean ± SEM. One-way ANOVA followed by Tukey's post hoc test.

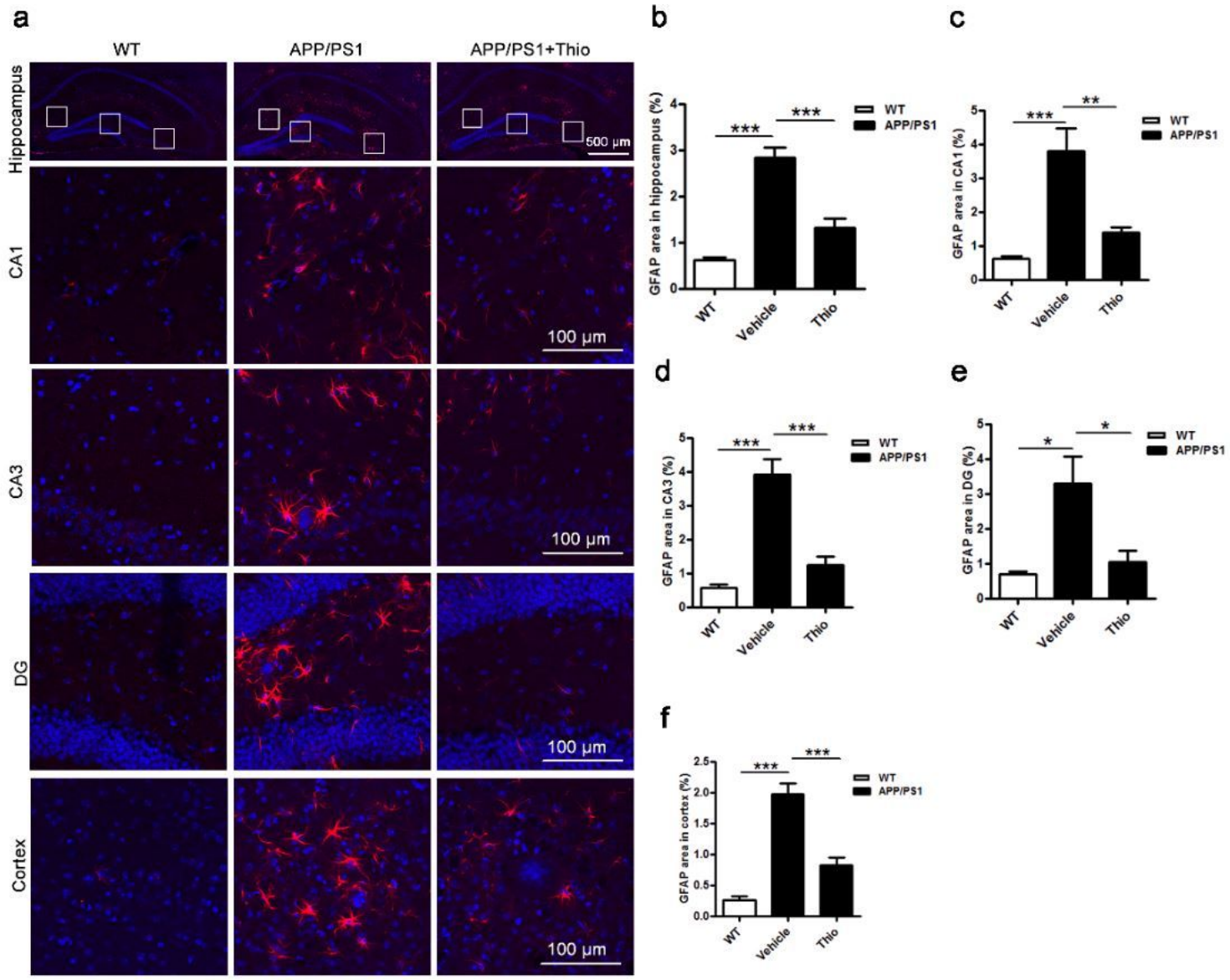


## Figure 2

Effect of thioperamide on astrocytic reactivity in APP/PS1 Tg mice. a-f Representative immunohistochemical staining of GFAP (red) and bar graph in either hippocampus (a, b), including CA1 (a, c), CA3 (a, d) and DG (a, e) or cortex (a, f) showing the GFAP+ astrocytic reactivity in those receiving vehicle and thioperamide in WT and APP/PS1 Tg mice. Scale bar: 100 μm. n = 5 per group. *P <0.05, **P <0.01, ***P <0.001. Mean ± SEM. One-way ANOVA followed by Tukey's post hoc test.

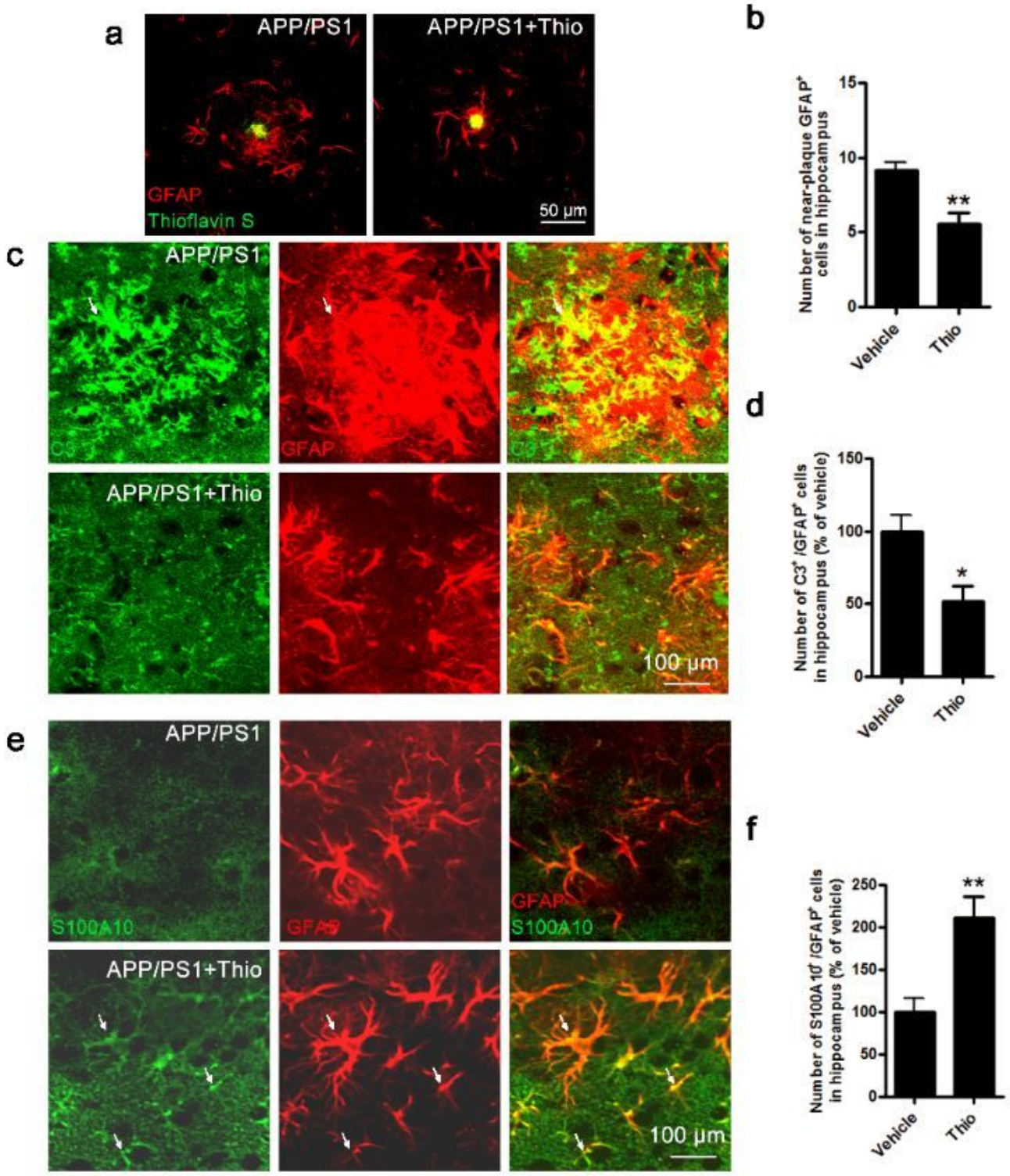


## Figure 3

Effects of thioperamide on near-plaque number of reactive astrocytes and influences on two astrocytic phenotypes in APP/PS1 Tg mice. a, b Representative immunohistochemical staining of GFAP (red) and bar graph in either hippocampus (a, b) or cortex (a, c) showing the numbers of near-plaque (≤ 50 μm, Thioflavin+) GFAP+ cells in those receiving vehicle and thioperamide in WT and APP/PS1 Tg mice. c, d Immunostaining of GFAP (red) and C3 (green) showing the effect of thioperamide on expression of A1-

type astrocytes. e, f Immunostaining of GFAP (red) and S100A10 (green) showing the effect of thioperamide on expression of A2-type astrocytes. Scale bar: 100 μm. n = 5 per group. *P <0.05, **P <0.01. Mean ± SEM. One-way ANOVA followed by Tukey's post hoc test.

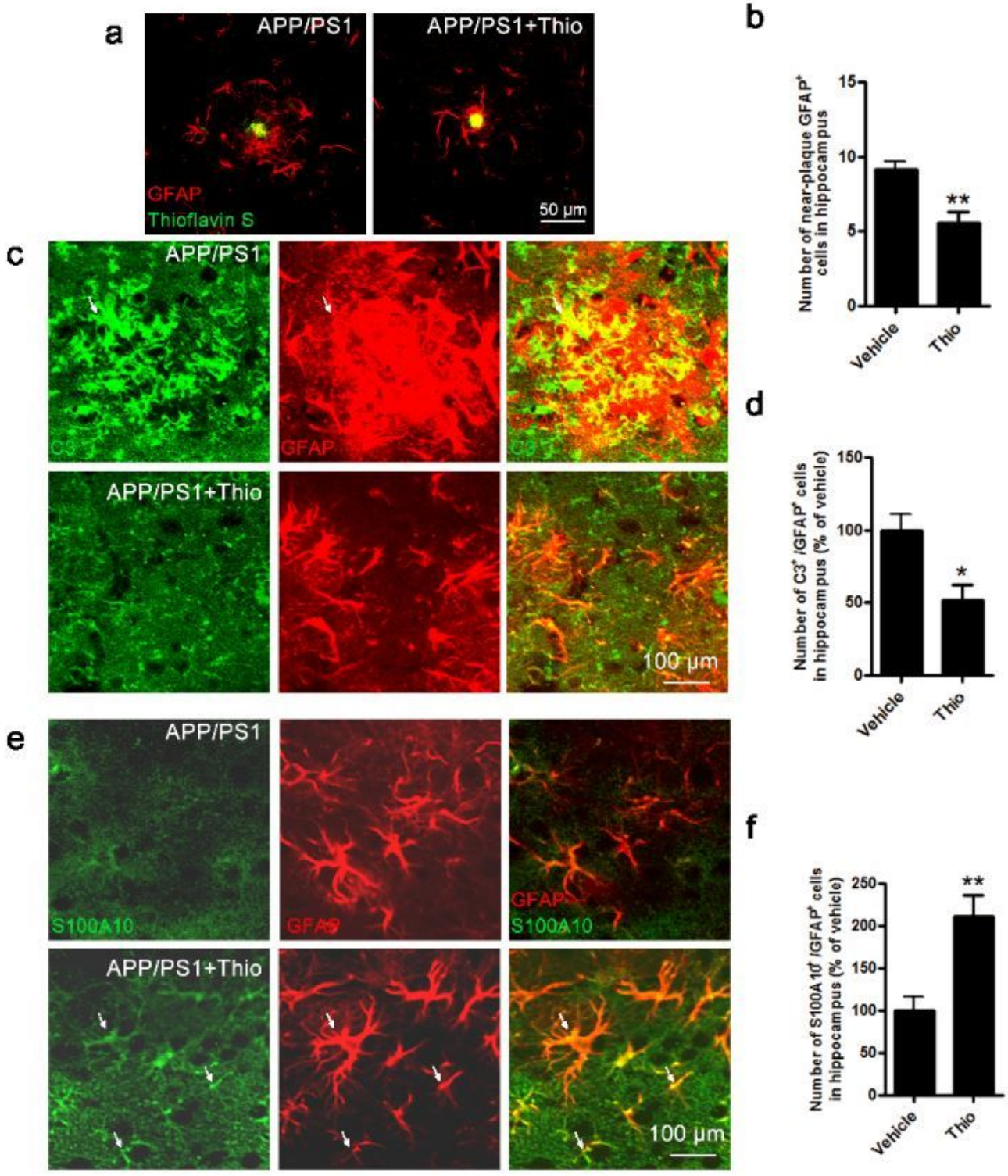


## Figure 3

Effects of thioperamide on near-plaque number of reactive astrocytes and influences on two astrocytic phenotypes in APP/PS1 Tg mice. a, b Representative immunohistochemical staining of GFAP (red) and

bar graph in either hippocampus (a, b) or cortex (a, c) showing the numbers of near-plaque (≤ 50 μm, Thioflavin+) GFAP+ cells in those receiving vehicle and thioperamide in WT and APP/PS1 Tg mice. c, d Immunostaining of GFAP (red) and C3 (green) showing the effect of thioperamide on expression of A1-type astrocytes. e, f Immunostaining of GFAP (red) and S100A10 (green) showing the effect of thioperamide on expression of A2-type astrocytes. Scale bar: 100 μm. n = 5 per group. *P <0.05, **P <0.01. Mean ± SEM. One-way ANOVA followed by Tukey's post hoc test.

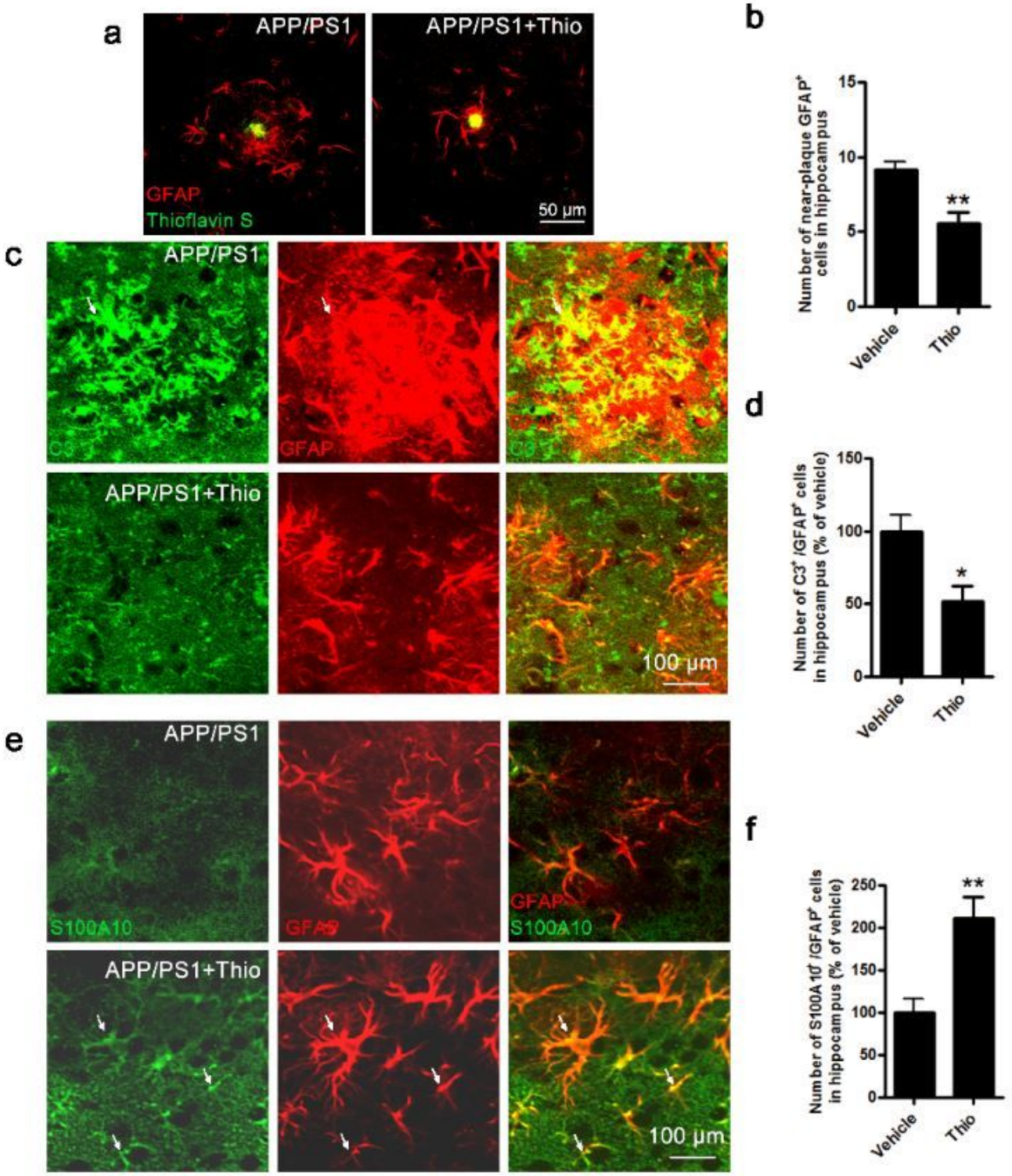


Figure 3

Effects of thioperamide on near-plaque number of reactive astrocytes and influences on two astrocytic phenotypes in APP/PS1 Tg mice. a, b Representative immunohistochemical staining of GFAP (red) and bar graph in either hippocampus (a, b) or cortex (a, c) showing the numbers of near-plaque (≤ 50 μm, Thioflavin+) GFAP+ cells in those receiving vehicle and thioperamide in WT and APP/PS1 Tg mice. c, d Immunostaining of GFAP (red) and C3 (green) showing the effect of thioperamide on expression of A1-type astrocytes. e, f Immunostaining of GFAP (red) and S100A10 (green) showing the effect of thioperamide on expression of A2-type astrocytes. Scale bar: 100 μm. n = 5 per group. *P <0.05, **P <0.01. Mean ± SEM. One-way ANOVA followed by Tukey's post hoc test.

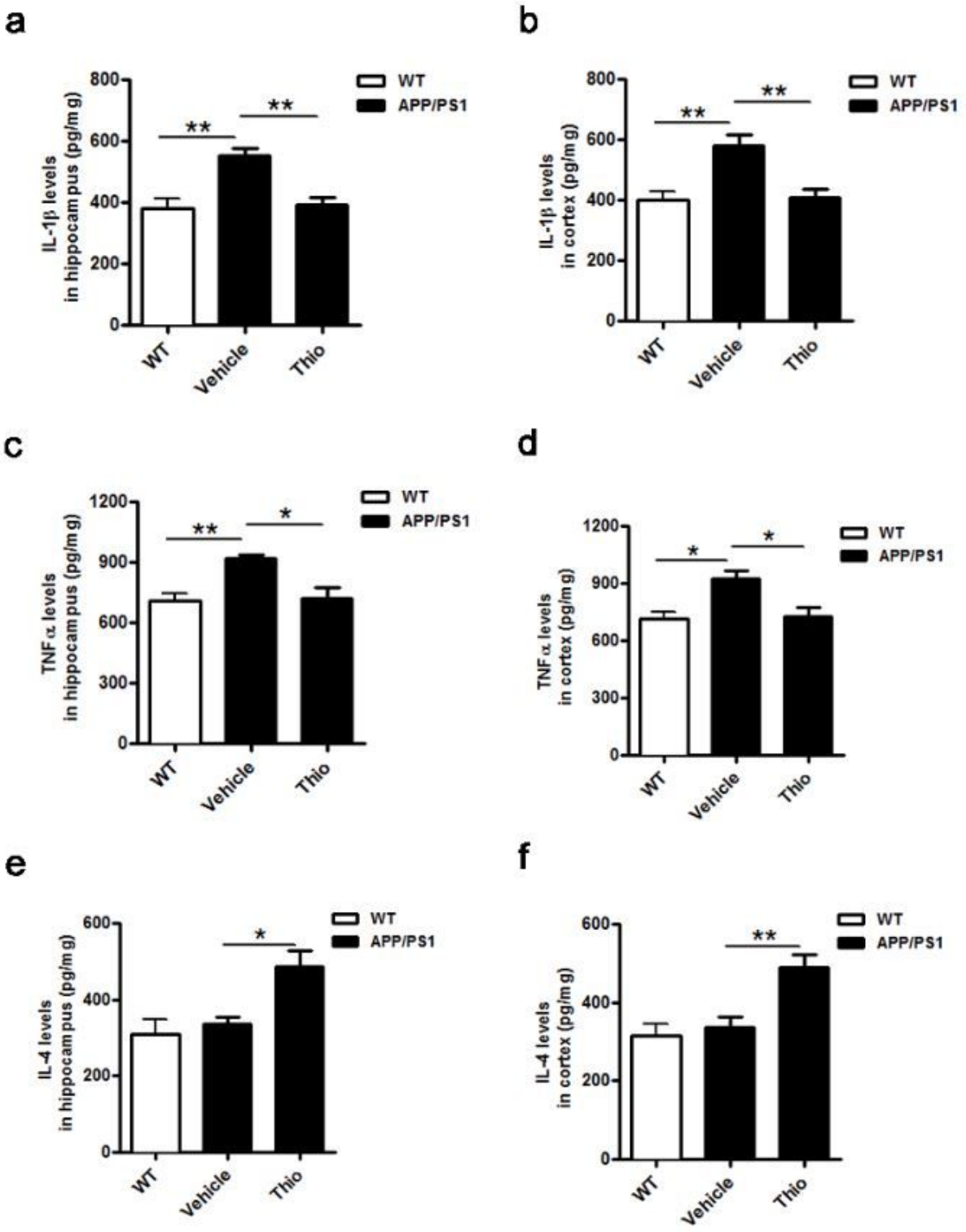


## Figure 4

Thioperamide treatment decreases proinflammatory cytokine production in APP/PS1 Tg mice. a-f IL-1β (a, b), TNF-α (c, d) and IL-4 (e, f) levels in the hippocampus and cortex were measured via ELISA in those receiving vehicle and thioperamide in WT and APP/PS1 Tg mice. n = 5 per group. *P <0.05, **P <0.01. Mean ± SEM. One-way ANOVA followed by Tukey's post hoc test.

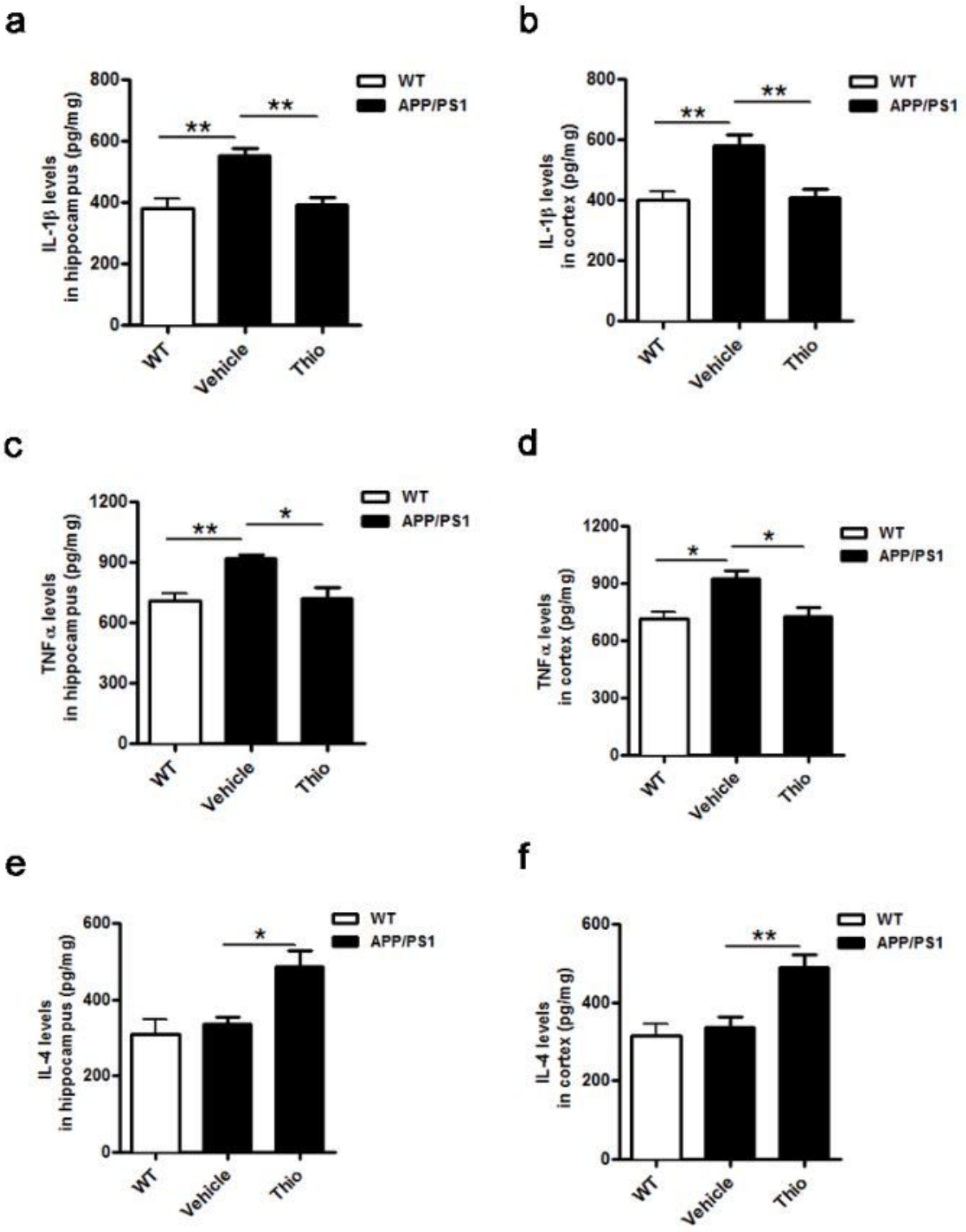


## Figure 4

Thioperamide treatment decreases proinflammatory cytokine production in APP/PS1 Tg mice. a-f IL-1β (a, b), TNF-α (c, d) and IL-4 (e, f) levels in the hippocampus and cortex were measured via ELISA in those receiving vehicle and thioperamide in WT and APP/PS1 Tg mice. n = 5 per group. *P <0.05, **P <0.01. Mean ± SEM. One-way ANOVA followed by Tukey's post hoc test.

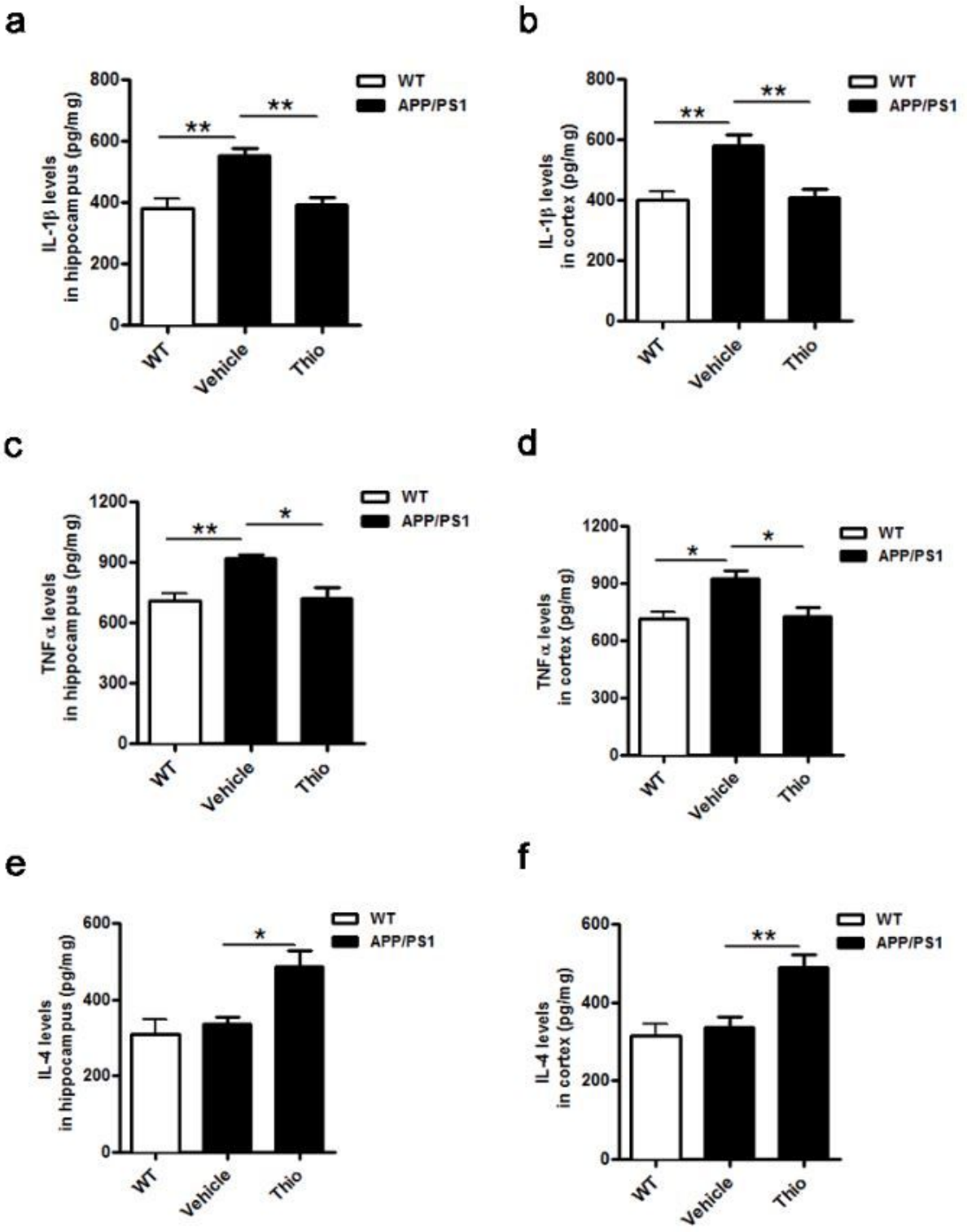


## Figure 4

Thioperamide treatment decreases proinflammatory cytokine production in APP/PS1 Tg mice. a-f IL-1β (a, b), TNF-α (c, d) and IL-4 (e, f) levels in the hippocampus and cortex were measured via ELISA in those receiving vehicle and thioperamide in WT and APP/PS1 Tg mice. n = 5 per group. *P <0.05, **P <0.01. Mean ± SEM. One-way ANOVA followed by Tukey's post hoc test.

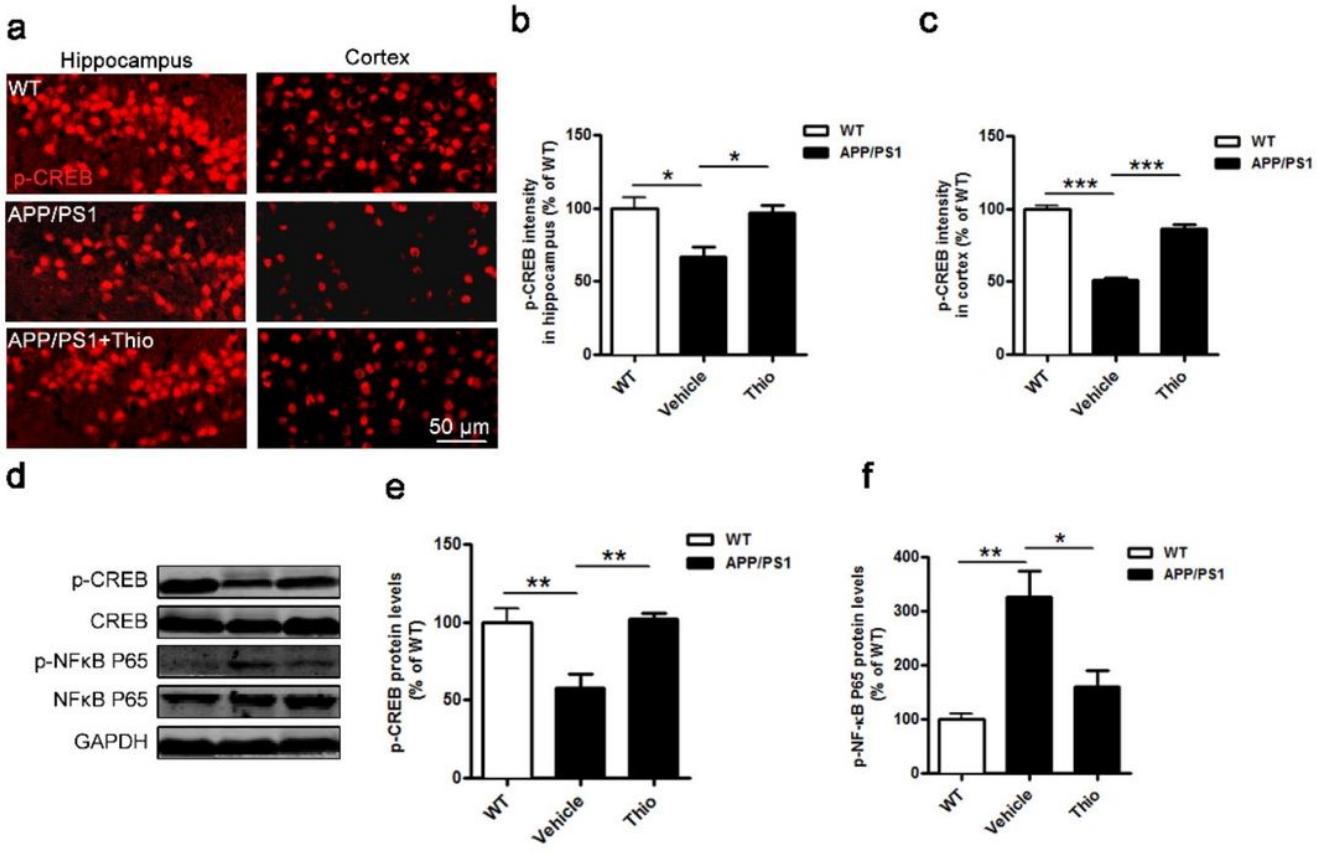


## Figure 5

Effects of thioperamide on levels of p-CREB and p-P65 NF-κB in APP/PS1 Tg mice. a-c Representative immunostaining by p-CREB (red) and bar graph in both hippocampus (a, b) and cortex (a, c) showing the activation of CREB in those receiving vehicle and thioperamide in WT and APP/PS1 Tg mice. Scale bar: 50 μm. d, e Representative Western blots and bar graph showing the effect of thioperamide on p-CREB (d, e) and p-P65 NF-κB (d, f) expression in hippocampus in WT and APP/PS1 Tg mice. n = 5 per group. *P <0.05, **P <0.01, ***P <0.001. Mean ± SEM. One-way ANOVA followed by Tukey's post hoc test.

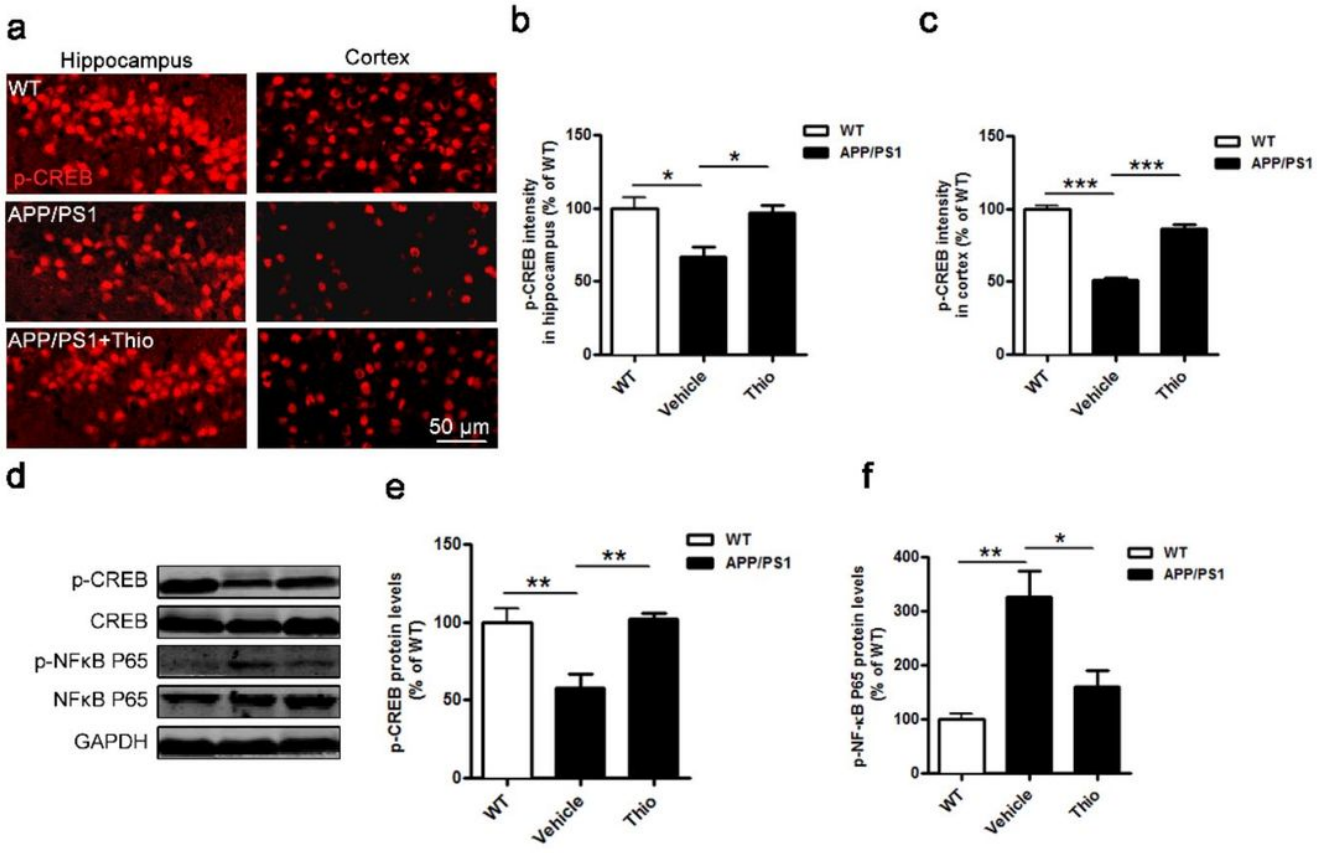


## Figure 5

Effects of thioperamide on levels of p-CREB and p-P65 NF-κB in APP/PS1 Tg mice. a-c Representative immunostaining by p-CREB (red) and bar graph in both hippocampus (a, b) and cortex (a, c) showing the activation of CREB in those receiving vehicle and thioperamide in WT and APP/PS1 Tg mice. Scale bar: 50 μm. d, e Representative Western blots and bar graph showing the effect of thioperamide on p-CREB (d, e) and p-P65 NF-κB (d, f) expression in hippocampus in WT and APP/PS1 Tg mice. n = 5 per group. *P <0.05, **P <0.01, ***P <0.001. Mean ± SEM. One-way ANOVA followed by Tukey's post hoc test.

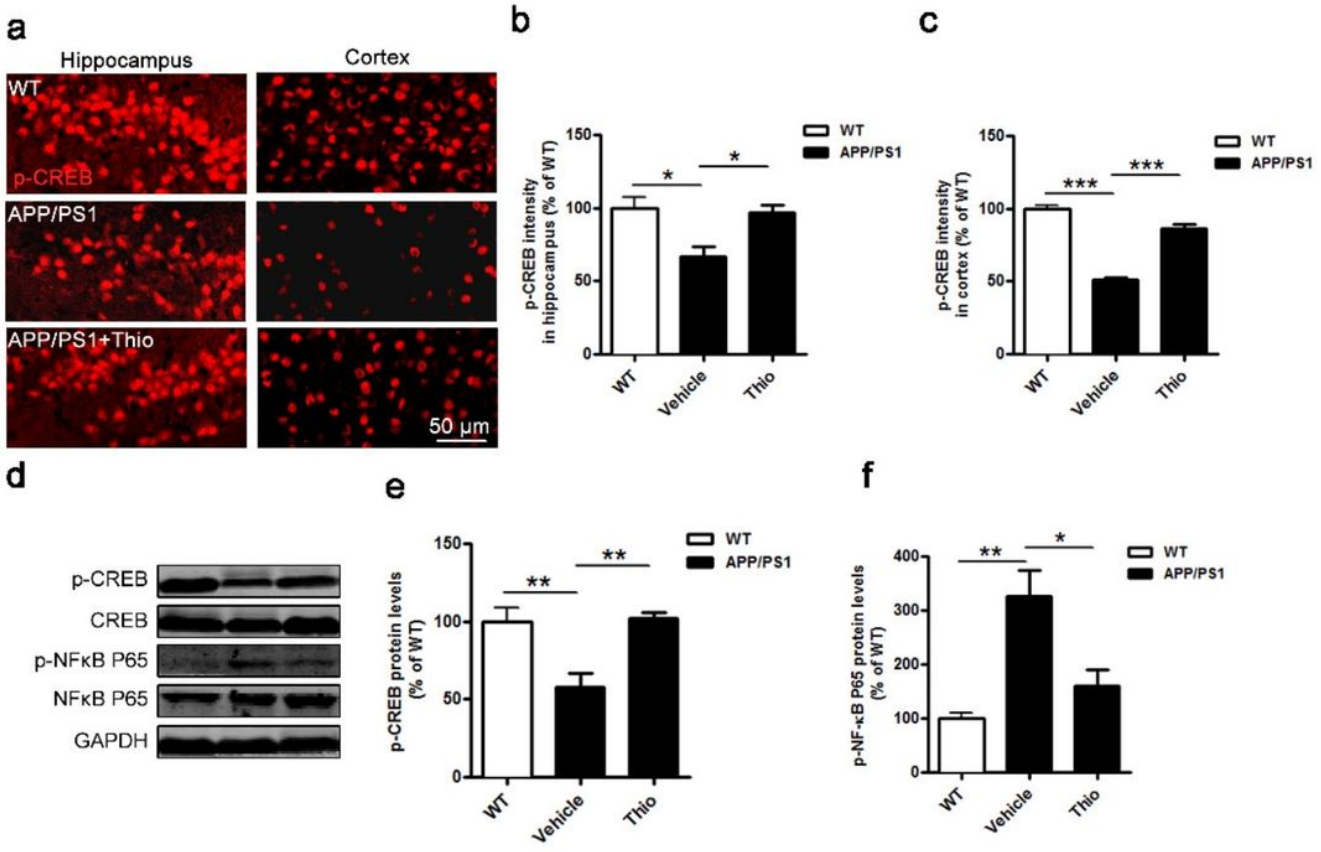


## Figure 5

Effects of thioperamide on levels of p-CREB and p-P65 NF-κB in APP/PS1 Tg mice. a-c Representative immunostaining by p-CREB (red) and bar graph in both hippocampus (a, b) and cortex (a, c) showing the activation of CREB in those receiving vehicle and thioperamide in WT and APP/PS1 Tg mice. Scale bar: 50 μm. d, e Representative Western blots and bar graph showing the effect of thioperamide on p-CREB (d, e) and p-P65 NF-κB (d, f) expression in hippocampus in WT and APP/PS1 Tg mice. n = 5 per group. *P <0.05, **P <0.01, ***P <0.001. Mean ± SEM. One-way ANOVA followed by Tukey's post hoc test.

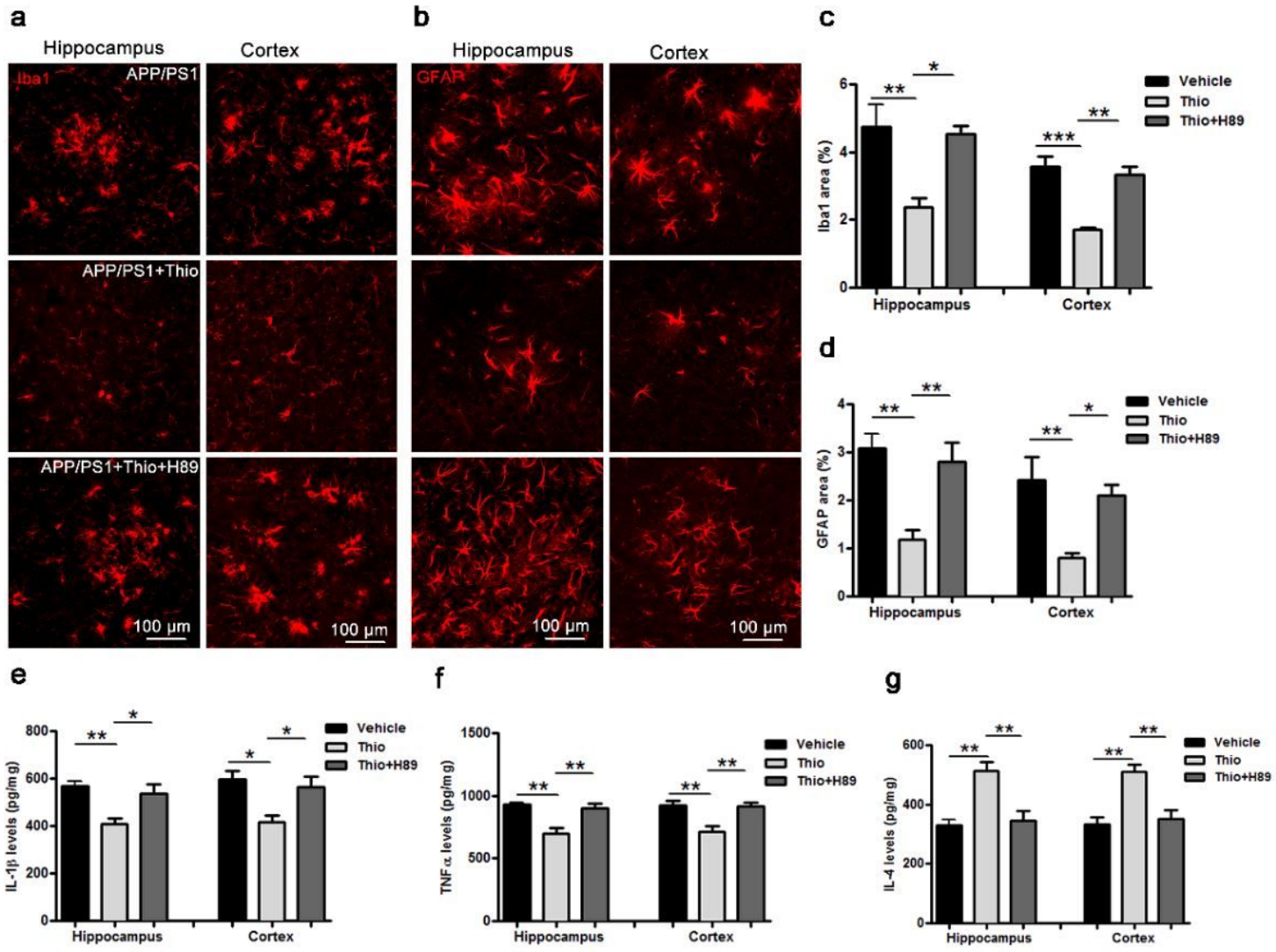


## Figure 6

Inhibition of CREB activity reverses the reduced gliosis and inflammatory response by thioperamide in APP/PS1 Tg mice. a-d Representative immunostaining (a, b) and bar graph (c, d) of Iba1 (red) (a, c) and GFAP (red) (b, d) in both hippocampus and cortex showing the effect of H89 on inhibition of microgliosis and astrogliosis offered by thioperamide in APP/PS1 Tg mice. Scale bar: 100 μm. e-g IL-1β (e), TNF-α (f) and IL-4 (g) levels in both hippocampus and cortex were measured via ELISA in those receiving H89 and thioperamide in APP/PS1 Tg mice. n = 5 per group. *P <0.05, **P <0.01, ***P <0.001. Mean ± SEM. One-way ANOVA followed by Tukey's post hoc test.

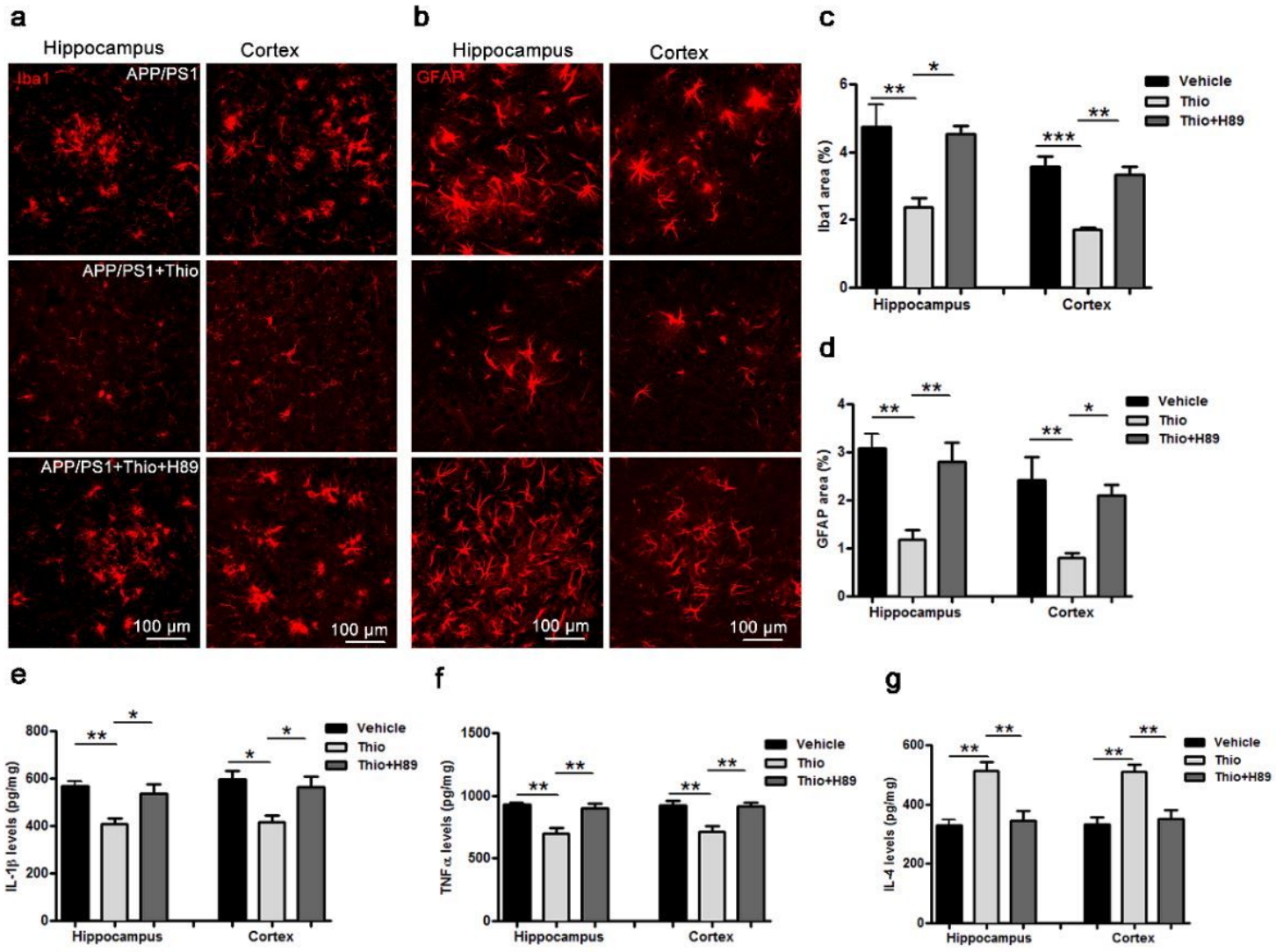


## Figure 6

Inhibition of CREB activity reverses the reduced gliosis and inflammatory response by thioperamide in APP/PS1 Tg mice. a-d Representative immunostaining (a, b) and bar graph (c, d) of Iba1 (red) (a, c) and GFAP (red) (b, d) in both hippocampus and cortex showing the effect of H89 on inhibition of microgliosis and astrogliosis offered by thioperamide in APP/PS1 Tg mice. Scale bar: 100 μm. e-g IL-1β (e), TNF-α (f) and IL-4 (g) levels in both hippocampus and cortex were measured via ELISA in those receiving H89 and thioperamide in APP/PS1 Tg mice. n = 5 per group. *P <0.05, **P <0.01, ***P <0.001. Mean ± SEM. One-way ANOVA followed by Tukey's post hoc test.

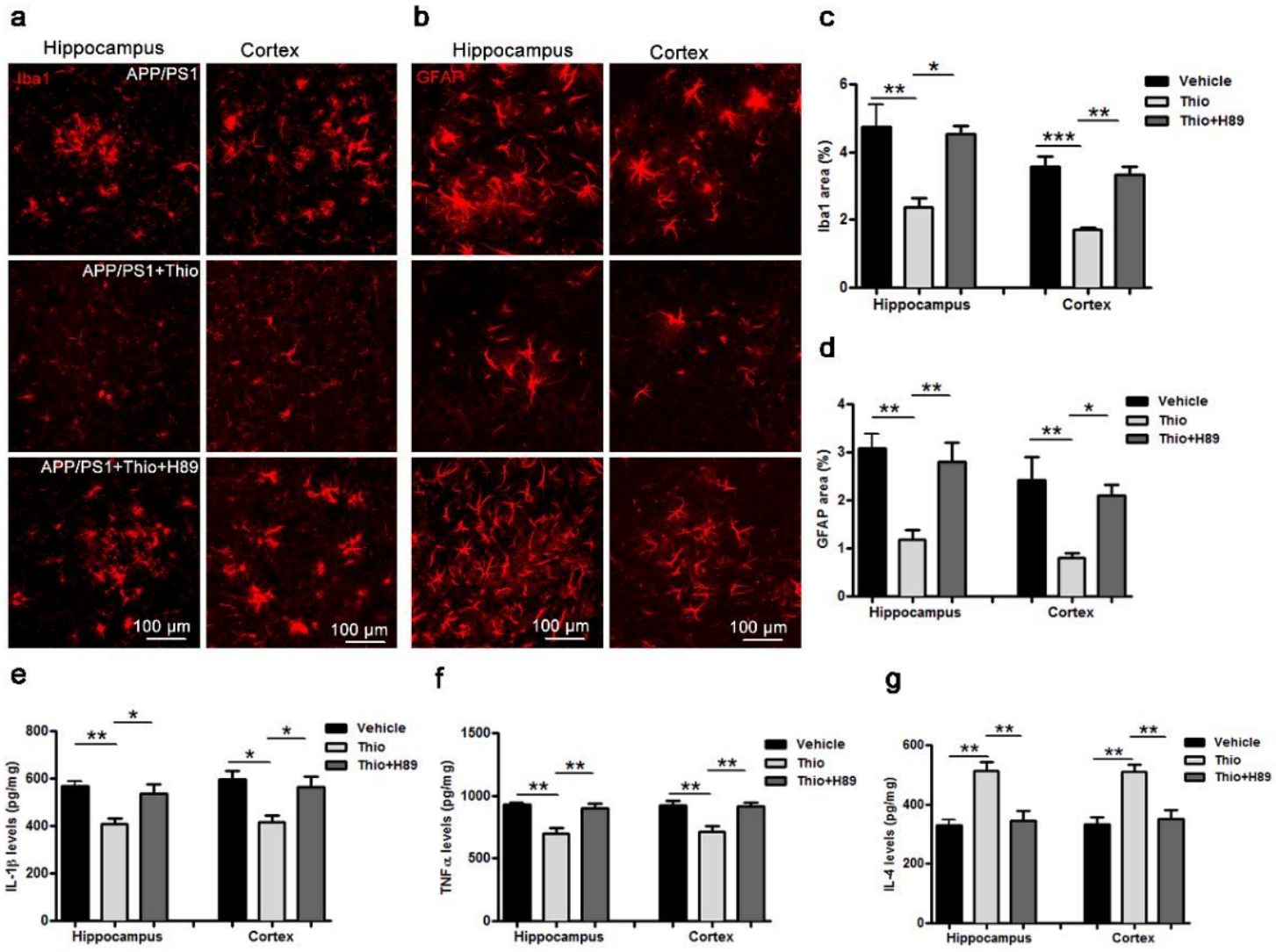


## Figure 6

Inhibition of CREB activity reverses the reduced gliosis and inflammatory response by thioperamide in APP/PS1 Tg mice. a-d Representative immunostaining (a, b) and bar graph (c, d) of Iba1 (red) (a, c) and GFAP (red) (b, d) in both hippocampus and cortex showing the effect of H89 on inhibition of microgliosis and astrogliosis offered by thioperamide in APP/PS1 Tg mice. Scale bar: 100 μm. e-g IL-1β (e), TNF-α (f) and IL-4 (g) levels in both hippocampus and cortex were measured via ELISA in those receiving H89 and thioperamide in APP/PS1 Tg mice. n = 5 per group. *P <0.05, **P <0.01, ***P <0.001. Mean ± SEM. One-way ANOVA followed by Tukey's post hoc test.

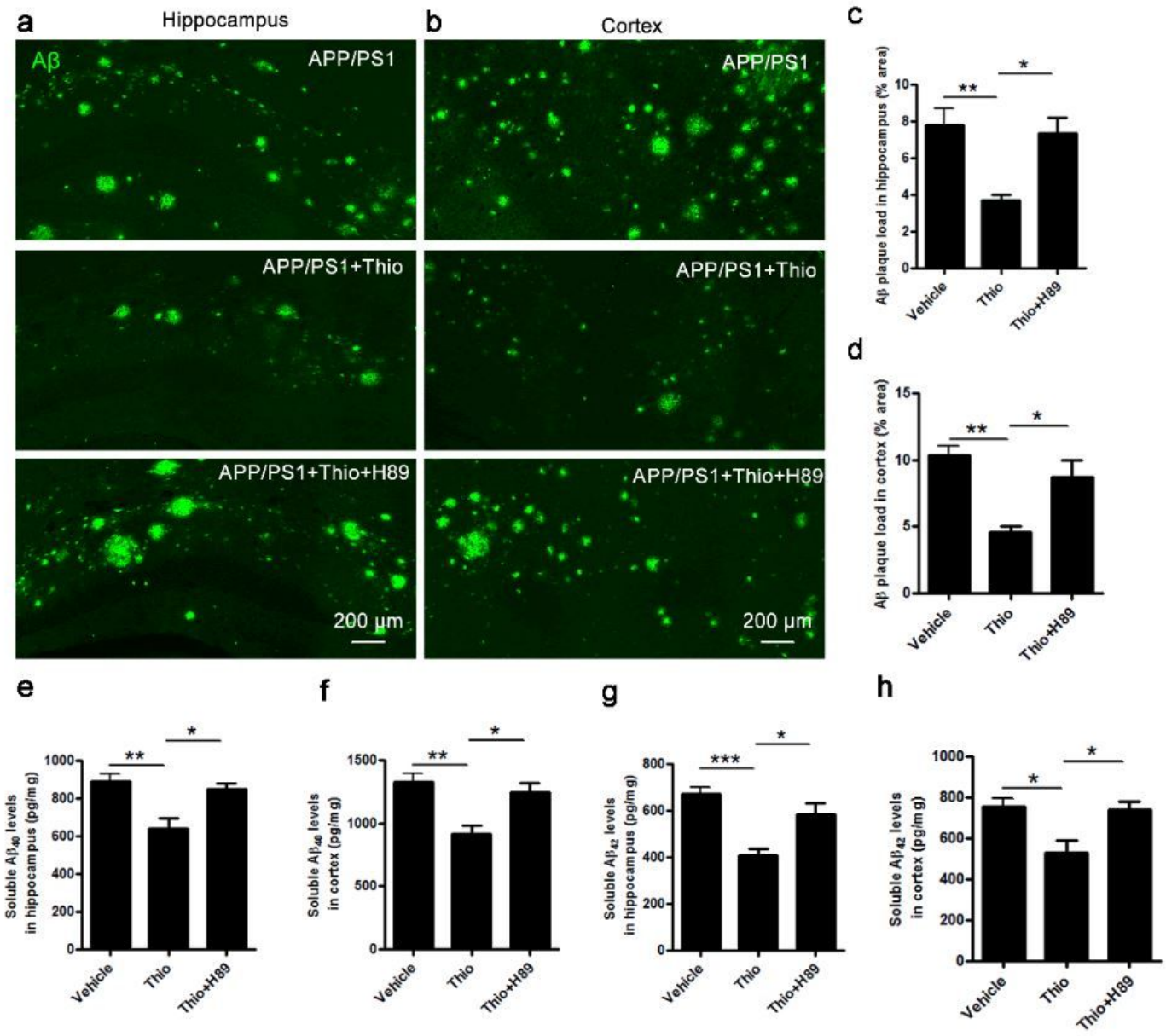


## Figure 7

H89 reverses the reduced A pathology by thioperamide in APP/PS1 Tg mice. a-d Representative immunohistochemical staining of Aβ and bar graph in both hippocampus (a, c) and cortex (b, d) showing the deposition of Aβ in those receiving vehicle, thioperamide and H89 in APP/PS1 Tg mice. Scale bar: 200 μm. e-h soluble Aβ40 (e, f) and Aβ42 (g, h) levels in both hippocampus (e, g) and cortex (f, h) were measured via ELISA in those receiving H89 and thioperamide in APP/PS1 Tg mice. n = 5 per group. *P <0.05, **P <0.01, ***P <0.001. Mean ± SEM. One-way ANOVA followed by Tukey's post hoc test.

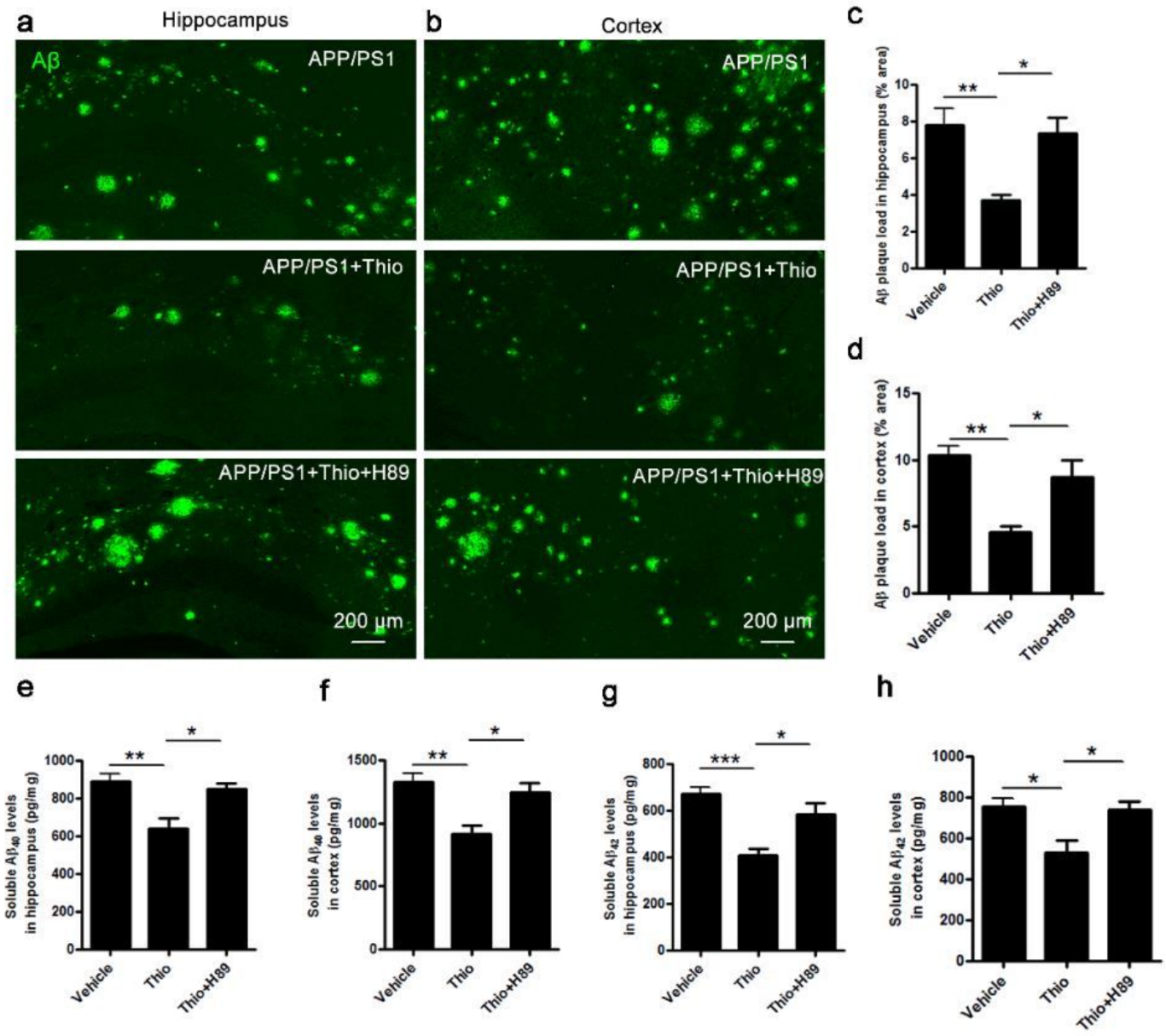


## Figure 7

H89 reverses the reduced A pathology by thioperamide in APP/PS1 Tg mice. a-d Representative immunohistochemical staining of Aβ and bar graph in both hippocampus (a, c) and cortex (b, d) showing the deposition of Aβ in those receiving vehicle, thioperamide and H89 in APP/PS1 Tg mice. Scale bar: 200 μm. e-h soluble Aβ40 (e, f) and Aβ42 (g, h) levels in both hippocampus (e, g) and cortex (f, h) were measured via ELISA in those receiving H89 and thioperamide in APP/PS1 Tg mice. n = 5 per group. *P <0.05, **P <0.01, ***P <0.001. Mean ± SEM. One-way ANOVA followed by Tukey's post hoc test.

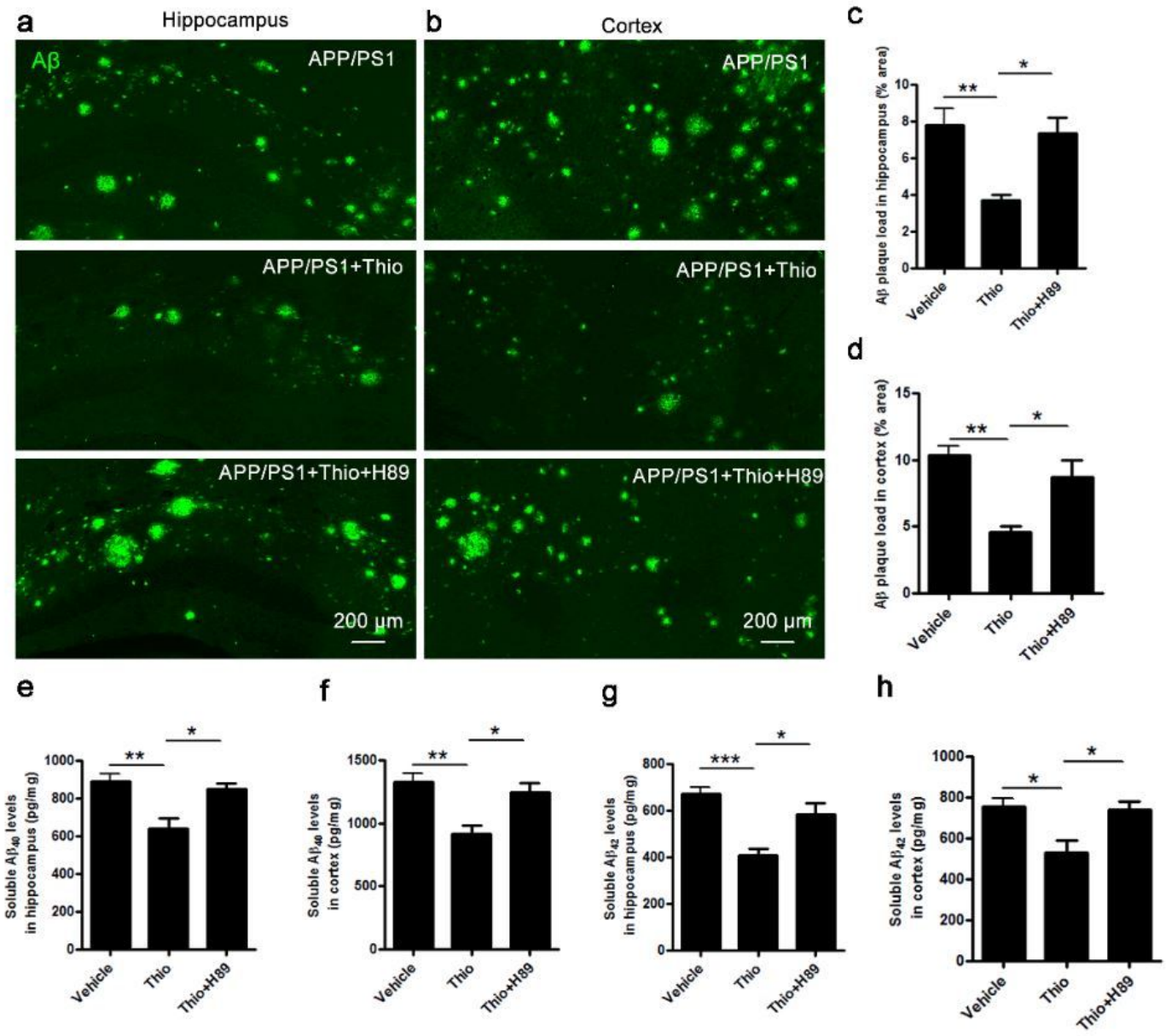


## Figure 7

H89 reverses the reduced A pathology by thioperamide in APP/PS1 Tg mice. a-d Representative immunohistochemical staining of Aβ and bar graph in both hippocampus (a, c) and cortex (b, d) showing the deposition of Aβ in those receiving vehicle, thioperamide and H89 in APP/PS1 Tg mice. Scale bar: 200 μm. e-h soluble Aβ40 (e, f) and Aβ42 (g, h) levels in both hippocampus (e, g) and cortex (f, h) were measured via ELISA in those receiving H89 and thioperamide in APP/PS1 Tg mice. n = 5 per group. *P <0.05, **P <0.01, ***P <0.001. Mean ± SEM. One-way ANOVA followed by Tukey's post hoc test.

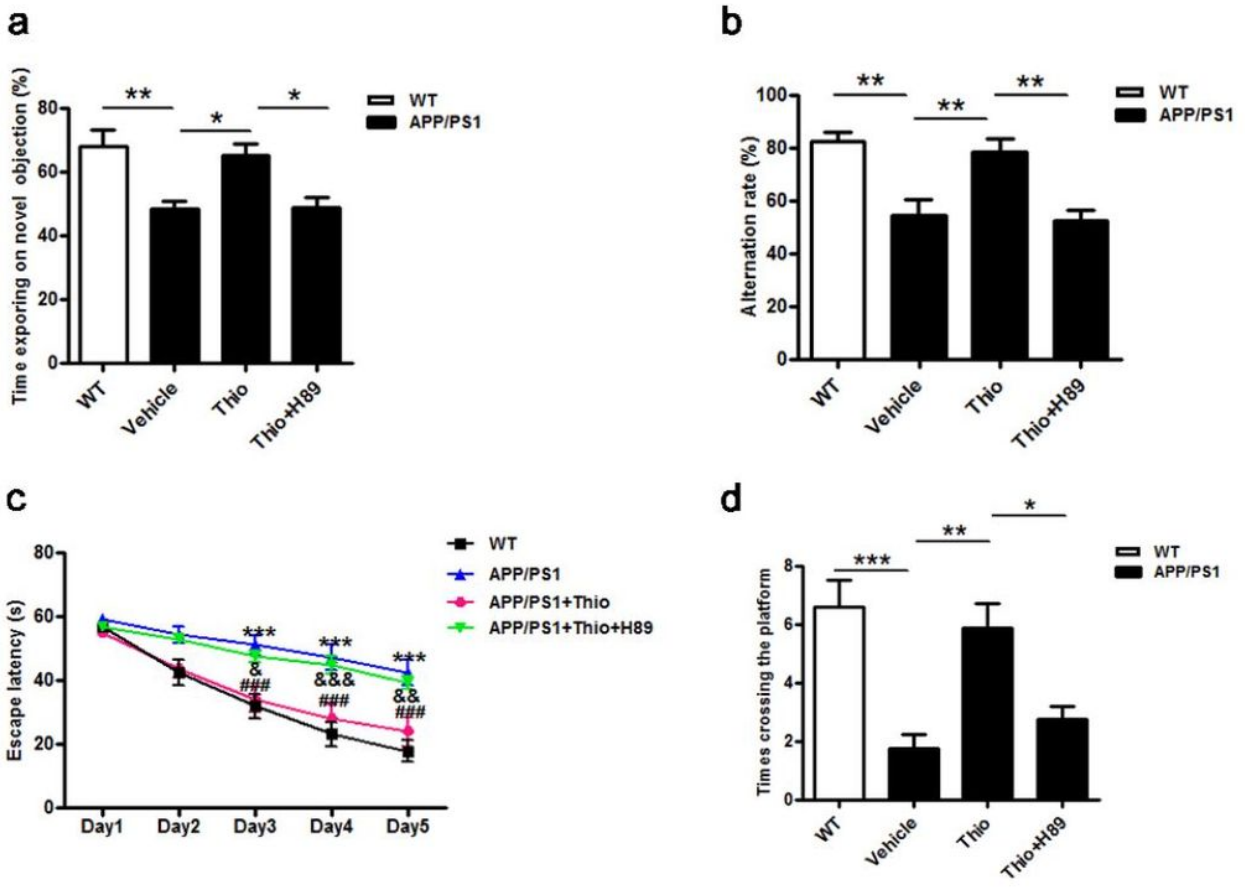


## Figure 8

H89 reverses the ameliorated cognitive dysfunction by thioperamide in APP/PS1 Tg mice. a The NOR test showing effect of H89 and thioperamide on the exploring time on new object in WT and APP/PS1 Tg mice. b The Y maze test showing the alternation rate in those receiving vehicle, thioperamide, and H89 in WT and APP/PS1 Tg mice. c, d The MWM test showing the escape latency on training days (c) and crossing times on testing day (d) in those receiving vehicle, thioperamide, and H89 in WT and APP/PS1 Tg mice. n = 8 per group. *P <0.05, **P <0.01, ***P <0.001 in a, b and d. ***P <0.001 vs. the WT group; ###P <0.001 vs. the vehicle treated APP/PS1 Tg group; &P <0.05, &&P <0.01, &&&P <0.001 vs. the thioperamide treated APP/PS1 Tg group in group in c. Mean ± SEM. One-way ANOVA followed by Tukey's post hoc (a, b, d) and two-way ANOVA followed by Bonferroni post hoc test (c).

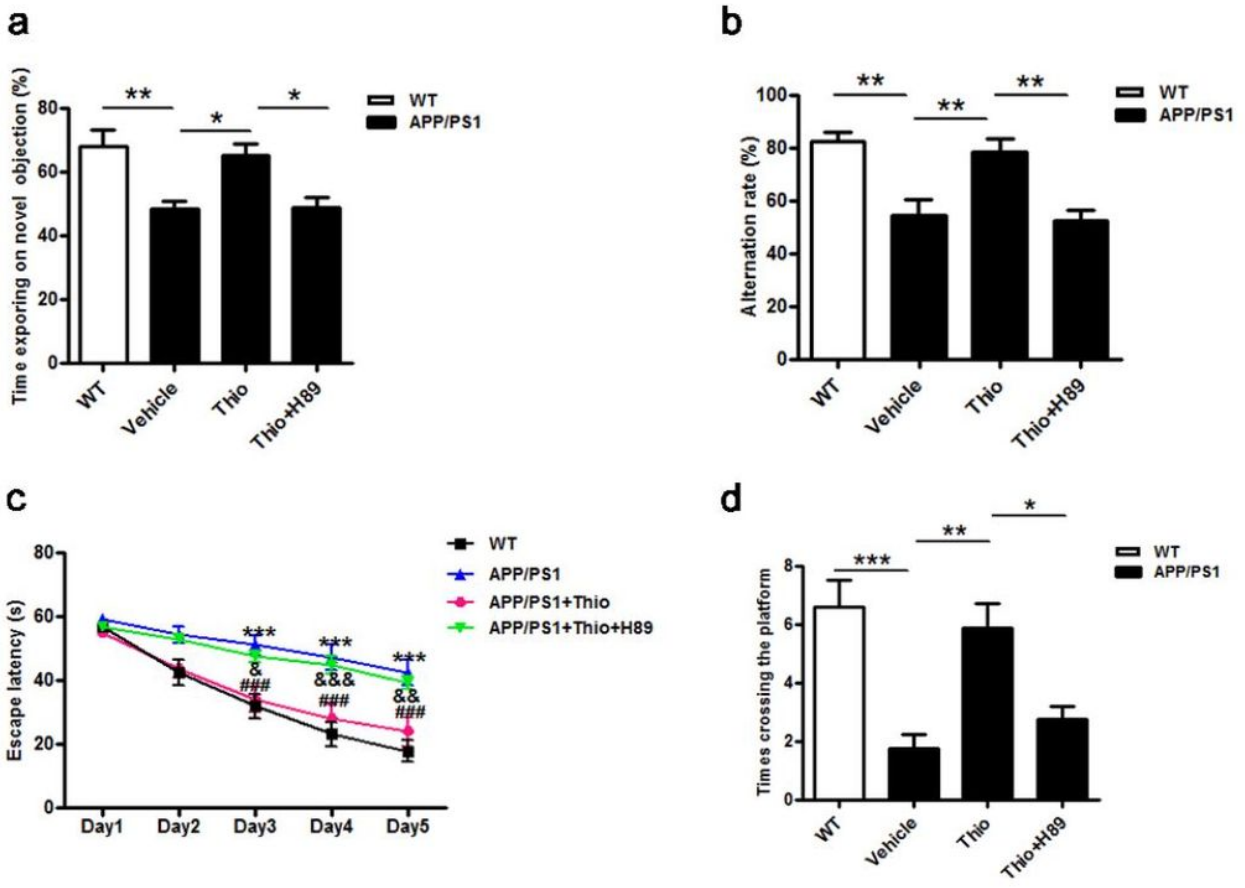


## Figure 8

H89 reverses the ameliorated cognitive dysfunction by thioperamide in APP/PS1 Tg mice. a The NOR test showing effect of H89 and thioperamide on the exploring time on new object in WT and APP/PS1 Tg mice. b The Y maze test showing the alternation rate in those receiving vehicle, thioperamide, and H89 in WT and APP/PS1 Tg mice. c, d The MWM test showing the escape latency on training days (c) and crossing times on testing day (d) in those receiving vehicle, thioperamide, and H89 in WT and APP/PS1 Tg mice. n = 8 per group. *P <0.05, **P <0.01, ***P <0.001 in a, b and d. ***P <0.001 vs. the WT group; ###P <0.001 vs. the vehicle treated APP/PS1 Tg group; &P <0.05, &&P <0.01, &&&P <0.001 vs. the thioperamide treated APP/PS1 Tg group in group in c. Mean ± SEM. One-way ANOVA followed by Tukey's post hoc (a, b, d) and two-way ANOVA followed by Bonferroni post hoc test (c).

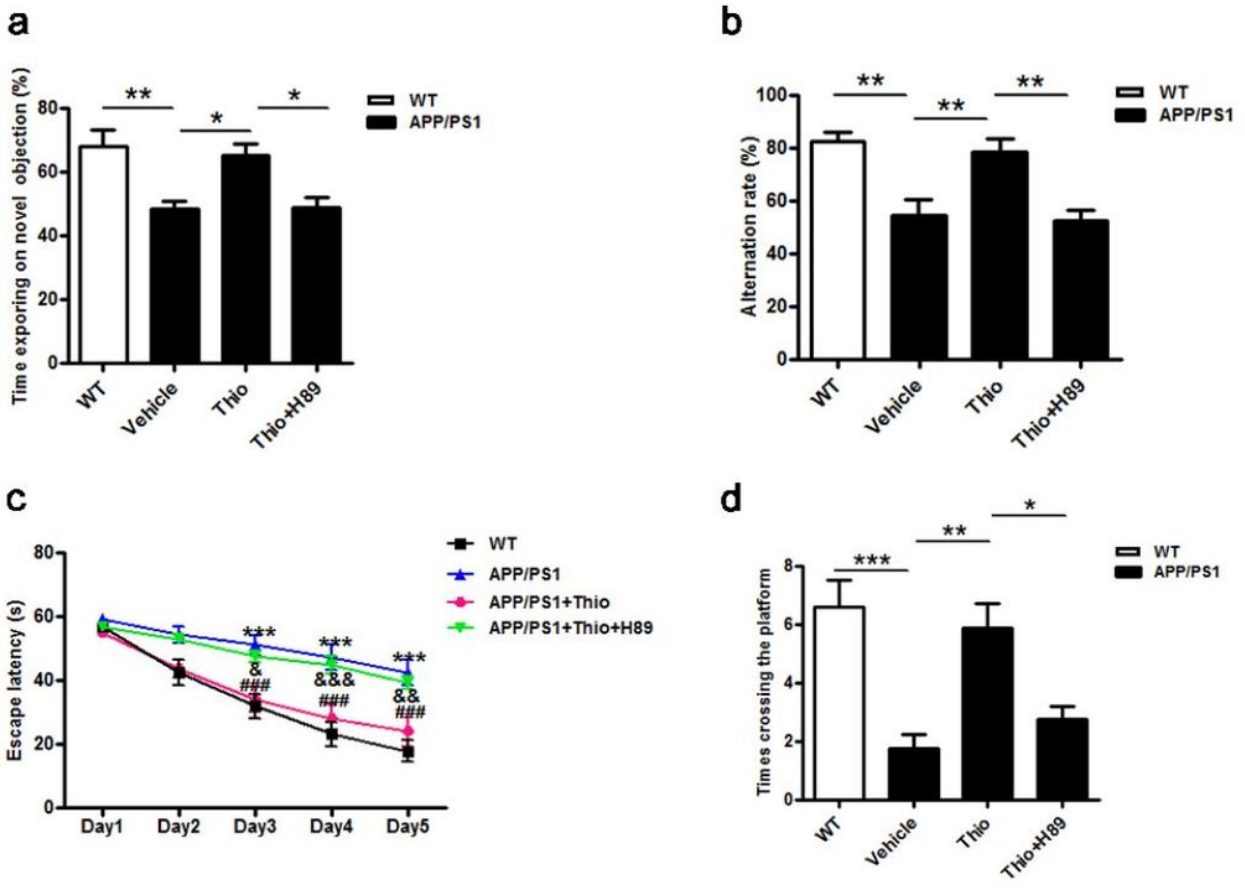


## Figure 8

H89 reverses the ameliorated cognitive dysfunction by thioperamide in APP/PS1 Tg mice. a The NOR test showing effect of H89 and thioperamide on the exploring time on new object in WT and APP/PS1 Tg mice. b The Y maze test showing the alternation rate in those receiving vehicle, thioperamide, and H89 in WT and APP/PS1 Tg mice. c, d The MWM test showing the escape latency on training days (c) and crossing times on testing day (d) in those receiving vehicle, thioperamide, and H89 in WT and APP/PS1 Tg mice. n = 8 per group. *P <0.05, **P <0.01, ***P <0.001 in a, b and d. ***P <0.001 vs. the WT group; ###P <0.001 vs. the vehicle treated APP/PS1 Tg group; &P <0.05, &&P <0.01, &&&P <0.001 vs. the thioperamide treated APP/PS1 Tg group in group in c. Mean ± SEM. One-way ANOVA followed by Tukey's post hoc (a, b, d) and two-way ANOVA followed by Bonferroni post hoc test (c).